Published in final edited form as:
Curr Radiopharm. 2008 September 1; 1(3): 177.

Astatine Radiopharmaceuticals: Prospects and Problems

Ganesan Vaidyanathan* and **Michael R. Zalutsky**
Department of Radiology, Duke University Medical Center, Durham, North Carolina, USA

Abstract

For the treatment of minimum residual diseases such micrometastases and residual tumor margins that remain after debulking of the primary tumor, targeted radiotherapy using radiopharmaceuticals tagged with α-particle-emitting radionuclides is very attractive. In addition to the their short range in tissue, which helps minimize harmful effects on adjacent normal tissues, α-particles, being high LET radiation, have several radiobiological advantages. The heavy halogen, astatine-211 is one of the prominent α-particle-emitting radionuclides in practice. Being a halogen, it can often be incorporated into biomolecules of interest by adapting radioiodination chemistry. A wide spectrum of compounds from the simple [^{211}At]astatide ion to small organic molecules, peptides, and large proteins labeled with ^{211}At have been investigated with at least two reaching the stage of clinical evaluation. The chemistry, cytotoxic advantages, biodistribution studies, and microdosimetry/pharmacokinetic modeling of some of these agents will be reviewed. In addition, potential problems such as the harmful effect of radiolysis on the synthesis, lack of sufficient *in vivo* stability of astatinated compounds, and possible adverse effects when they are systemically administered will be discussed.

INTRODUCTION

Targeted radionuclide therapy involves radiolabeled biomolecules and is a promising approach with which curative doses of radiation can be selectively delivered to tumors. Most targeted radionuclide therapeutic investigations employ radionuclides that emit β-particles such as ^{131}I and ^{90}Y. For example, ^{90}Y-labeled Zevalin® and ^{131}I-labeled Bexxar® are two FDA approved radiopharmaceuticals for the treatment of lymphoma [1,2]. Beta-particles have a long range in tissues and therefore deposit their energy over several millimeters. As a result of this, the fraction of absorbed radiation dose in tumor decreases with the decreasing size of the tumor. For example, it has been calculated that the ratio of fractional absorbed dose from the α-particle emitter ^{211}At to that from ^{90}Y will be 9 and 33 for a 1000 μm and 200 μm diameter tumors, respectively [3]. Thus β-particles are appropriate for the treatment of larger tumors. The long β-particle range is advantageous because it can help compensate for heterogeneous radiopharmaceutical uptake; however, this property can also lead to detrimental irradiation of normal tissues adjacent to smaller tumors.

On the other hand, the short range α-particles are ideal for the treatment of minimal residual diseases, settings in which the targeted radiotherapy has the greatest chance of success [4]. Such diseases include micrometastatic lesions, residual tumor margins that remain after debulking the primary tumor by surgery, and tumors in circulation including lymphoma and leukemia. In addition, targeted alpha particle therapy may be ideal for ovarian cancer and

*Address correspondence to this author at the Box 3808, Radiology, Duke University Medical Center, Durham, North Carolina 27710, USA; Tel: (919) 684-7811; Fax: (919) 684-7122; ganesan.v@duke.edu.

neoplastic meningitis, which spread as thin sheets of compartmentalalized tumor often accompanied by free-floating cells.

Due to their short range and high energy, α-particles are radiation of high linear energy transfer (LET). This property offers a number of radiobiological advantages [5]: 1) Their relative biological effectiveness is very high. This is due to the fact that the average separation between ionizing events at this ionization density nearly coincides with the diameter of the DNA double helix, increasing the probability of double-strand breaks. 2) Because of the higher probability for creating double-DNA-strand breaks, which are generally not repairable [6], the cytotoxic effectiveness of α-particles is much less dependent on dose rate compared with β-particles. This is an important advantage since in many cases, the dose rates achieved with targeted radiotherapy have not been high. 3) Another advantage of high-LET radiation is that their oxygen enhancement ratio is nearly unity making it possible to treat both normoxic and hypoxic cell populations. 4) Finally, the cytotoxic effect of high-LET radiation does not depend on the cell cycle status [5].

There are about 100 radionuclides that are known to decay by the emission of α-particles. However, a number of factors must be considered in choosing an α-particle emitter for a particular therapeutic application. It will be advantageous if the fraction of decays that yield α-particles is high and, for certain applications, there should be none or minimal β-particles emission. Emission of gamma rays or x-rays, which are suitable for imaging, will be a plus because it permits determination of pharmacokinetics and dosimetry of the labeled therapeutic. Other considerations in selecting an appropriate α-emitter include physical half life of the radionuclide, which ideally should match the biological half life of the radiotracer or its catabolites, ease of chemical synthesis and availability at a reasonable cost. Bismuth-212 [7], ^{213}Bi [8], ^{223}Ra [9], ^{225}Ac [10,11], and ^{211}At [12] are some of the most commonly investigated α-particle emitting radionuclides. A strong case can be made that ^{211}At is the most promising among these for the α-particle therapy. This review is focused on astatinated radiopharmaceuticals, especially covering the developments that have occurred since this area was reviewed previously [12-14].

ASTATINE-211

General

In 1869, the Russian chemist Dmitri Mendeleev predicted the existence of a fifth halogen and termed it *eka-iodine*. However, it wasn't discovered until 1940 when Corson *et al.* [15] produced it by the bombardment of ^{209}Bi with alpha particles and named it Astatine, which in Greek means unstable. Astatine-211 has a half life of 7.2 h and decays by a double branched pathway (Fig. **1**) producing one α-particle per decay. The first branch (42%) involves decay to ^{207}Bi *via* the emission of 5.87 MeV α-particles; the long half life of the daughter ^{207}Bi is not problematic because less than 0.001 ^{207}Bi decays occur per ^{211}At decay. The intermediate ^{207}Bi eventually decays to stable lead. The second branch (58%) is by electron capture to 520 ms ^{211}Po, which in turn de-excites by the emission of 7.45 MeV α-particles to stable lead. The mean ranges in tissue of the lower and higher energy α-particles emitted by ^{211}At are approximately 55 and 80 μm, respectively. The LET_{mean} of ^{211} At α-particles is about 100 keV/μm^{-1}, which is close to the value at which the relative biological effectiveness of ionizing radiation is highest [5]. The electron capture decay of ^{211}At to ^{211}Po emits polonium K x-rays which make it convenient to count ^{211}At activity levels and to perform scintigraphic imaging of ^{211}At uptake in tissues *in vivo* [16,17].

Production

Perhaps the major hurdle in the utilization of ^{211}At for radiotherapy is its lack of availability [18]. A medium-energy cyclotron with the capability of generating a 25-30 MeV α-particle beam is needed for its production. Unfortunately, there are currently not many institutions that have this kind of cyclotron. Astatine-211 is produced by the cyclotron bombardment of natural bismuth metal targets with 28–29 MeV α-particles *via* the ^{209}Bi(α, 2n)^{211}At reaction, followed by isolation of ^{211}At by dry distillation [19-24]. Care must be taken to minimize production of 8.1 h half life ^{210}At, which decays to ^{210}Po, an α-emitter with a 138 d half life. Polonium-210 is harmful to normal tissues especially to bone marrow because of its proclivity to bone uptake [25], and a method to assess this impurity in ^{211}At has been described [26]. For this reason, beam energies are kept below the threshold for the ^{209}Bi(α, 3n)^{210}At reaction during the production of ^{211}At [27]. Using internal cyclotron targets, up to 6.6 GBq of astatine-211 has been produced to date [28]. Typically, ^{211}At is isolated from the irradiated targets by dry distillation; however, other methods for its isolation have been explored [29,30].

Chemistry

Astatine belongs to the halogen family in the periodic table and has properties similar to that of other halogens; however, it does exhibit metallic characteristics as well [31-34]. A serious limitation of astatine with respect to chemical synthesis is that it does not have a stable isotope, preventing the characterization of astatinated compounds by common analytical techniques. Furthermore, the availability of a stable isotope also would have helped to further understand its redox chemistry and metallic behavior. Because carbon-halogen bond strength decreases with increasing atomic number of halogen [35,36], carbon-astatine bond is not remarkably strong. This can be detrimental in the use of astatinated radiopharmaceuticals because of the potential toxicity to normal organs like thyroid, bone marrow, spleen, stomach and lungs where released free astatide sequesters preferentially [37]. The carbon-halogen bond strength is higher when the halogen is attached to a *sp*2 carbon (aryl and vinyl) than when it is attached to a *sp*3 carbon [35]. For this reason, in most of the astatinated compounds investigated, the astatine is attached to an unactivated aromatic carbon. Attempts to introduce astatine on a vinylic carbon and the synthesis of vinyl-substituted astatinated steroid hormones have been reported [38-40].

In the early stages of development, aromatic astato compounds were synthesized by exchange halogenation [41-45] or by electrophilic substitution on unactivated [46] or activated aromatic rings [38,47,48]. Recently, a commonly used method for exchange radioiodination using copper catalysts has been adapted for astatination [49]. Low specific radioactivity is a serious limitation with exchange radiohalogenation and the presence of an activating group such a hydroxyl in phenols make the carbon-astatine bond further labile. Nucleophilic displacement of a diazonium moiety also has been used for the introduction of astatine onto an aromatic ring [50]. This method, however, results in multiple side products. The nucleophilic displacement of triazenes, a method used for radioiodination, has recently been utilized for astatination [51]. Currently, the most prevalent and versatile method is the electrophilic astatodemetallation of various organometallic derivatives, especially of organostannanes [52-58].

Due to the higher bond strength of boron-astatine bonds compared to carbon-astatine bonds, the use of *nido*-carborane and *closo*-dodecaborate (2-) for astatine labeling has been investigated [59] (see an accompanying article in this issue by Wilbur for more details). Labeling strategies that attempt to exploit the metallic character of the astatine atom through the formation of complexes of ^{211}At with chelating agents such as diethylenetriamine pentaacetic acid (DTPA) [60] and calix[4]arenes [61] have been reported. Likewise, labeling of antibodies *via* DTPA complexation also has been described [62-64]. The possibility of generating stable astatinated prosthetic groups by exploiting its soft anionic character has been

explored by attaching ^{211}At anion to soft metal cations such as mercury, rhodium, and iridium, which were complexed by bifunctional ligands [65-67].

SMALL MOLECULAR WEIGHT COMPOUNDS

[^{211}At]Astatide

Like iodide, astatide also accumulates in thyroid and stomach, and its uptake in macrophage-bearing organs such as spleen and lung is an order of magnitude higher than that of iodide [68]. Due to this proclivity, the simple [^{211}At]astatide ion may be suitable for the treatment cancers with upregulated sodium iodide symporter (NIS; see below). Such usefulness of [^{211}At]astatide has been investigated by determining its biodistribution in mice bearing subcutaneous anaplastic or follicular undifferentiated thyroid carcinomas; tumor accumulation of 11-28% of injected dose was observed [69-71]. Accumulation of iodide in the thyroid tissue is mediated by NIS, a membrane protein expressed on the basolateral surface of the thyrocyte. A recent study evaluated the biodistribution of free [^{211}At]-astatide and [^{125}I]iodide in mice bearing anaplastic thyroid carcinoma (ATC) and non tumor-bearing mice [72]. Except in thyroid, the uptake of [^{211}At]astatide was higher than that of [^{125}I]iodide in all tissues. Because the mean absorbed dose to normal tissues was higher than that to tumor tissues, the authors concluded that it may not be feasible to use [^{211}At]astatide for the treatment of ATC. The potential of simple radioiodide for the therapy of a variety of tumors transfected with the NIS gene has been explored. Due to the fast efflux of iodide from tumors, the physical half life of ^{131}I may not be suitable in treating tumors using this strategy. The 7.2 h half life of [^{211}At] astatide, on the other hand, is better matched to the egress kinetics of iodide observed in these tumors and therefore [^{211}At]astatide may be a better agent for this purpose. NIS-mediated uptake (Fig. **2**) and the potential utility of [^{211}At]astatide in the treatment of NIS-expressing tumors has been demonstrated [73,74]. In NIS-transfected glioma cells, the absorbed doses per unit administered radioactivity were 54- to 65-fold higher for [^{211}At]astatide than for [^{131}I] iodide. Both NIS-expressing and control cells showed increased sensitivity to ^{211}At over ^{131}I, with significantly lower D_0 (absorbed dose required to reduce the survival fraction to e^{-1}) and SF_2 (2-Gy survival fraction) values, highlighting the higher intrinsic cytotoxicity of alpha-particles. Petrich *et al.* also have demonstrated the potential advantages of [^{211}At] astatide for the treatment of NIS-expressing tumors [75,76]. Compared with nontransfected control cell lines, steady state radionuclide uptake in NIS-expressing cell lines increased up to 350-fold for ^{123}I, 340-fold for $^{99m}TcO_4^-$, and 60-fold for ^{211}At [75]; somewhat similar results also were obtained by scintigraphic imaging in xenograft models *in vivo*. Dosimetric calculations performed for ^{131}I and ^{211}At based on the scintigraphic data for ^{123}I and ^{211}At yielded tumor absorbed dose values of 3.5 Gy/MBq and 50.3 Gy/MBq for ^{131}I and ^{211}At, respectively. A follow up study evaluated the long term effects of [^{211}At]astatide in NIS-transfected tumor-bearing mice [76]. Complete eradication of the tumor was observed within three months in all cases with no tumor recurrence seen during 1 year follow up. Compared to a 40 day survival for the control group, 96% of the treated group survived after 6 month and 60% after 1 year. However, some side effects such as normal tissue damage and formation of secondary tumors were observed. Use of an anion channel blocker, 4,4′-diisothiocyanostilbene-2,2′-disulfonic acid (DIDS), to diminish the apical efflux of [^{211}At] astatide, thereby increasing its cellular retention has been investigated [77]. Employing an *in vitro* model of the thyroid follicular epithelium [78], it was shown that DIDS reduces the efflux of [^{211}At]astatide in cells prestimulated by thyroid stimulating hormone (TSH). On the contrary, unlike for iodide, in control cells and the cells treated with the mitogen EGF, there was a paradoxical increase in the retention of [^{211}At]astatide. Thus, it may be possible on the one hand to increase retention of [^{211}At]astatide in TSH stimulated tumor cells and on the other, reduce unwanted accumulation [^{211}At]astatide in the follicle lumen of intact thyroid during the treatment of extrathyroidal tumors.

Particulates

As described before, alpha particle therapy is suitable for tumors that grow as thin sheets on the surface of body cavities. Due to their relatively large size, particulate materials are less likely to leak out after direct administration within the cavity, and for this reason, colloids impregnated with ^{211}At have been investigated in an intraperitoneal ovarian tumor model [79,80]. Animals were cured with only 1-2 Bq of ^{211}At-tellurium colloid; in comparison, although three β-emitting radiocolloids prolonged median survival at activity levels of 296 MBq (^{165}Dy), 7.4 MBq (^{90}Y), and 5.6 MBq (^{32}P), no cures were obtained. These colloids were not pursued due to concerns of lack of their stability. Larsen *et al.* [81,82] have developed a stable form of the particulates by covalently linking [^{211}At]astatobenzoyl groups to monodisperse polymer particles (MDPP). After up to a 24 h incubation with fetal calf serum at room temperature, more than 90% of the radioactivity was still associated with MDPP. Significant prolongation in median survival was observed even at doses as low as 7 kBq of these ^{211}At-labeled mono-disperse polymer particles. Specific activities (MBq/mg) of the preparations did not influence the therapeutic efficacy and this was attributed to the larger size of these particles. From a study of ^{211}At-labeled human serum albumin microspheres B-20, it was found that in mice transplanted with malignant ascites, survival was prolonged in a dose-dependent manner; at a dose of 10 Gy, five out 16 animals survived [83]. Earlier, this group has reported the results from a clinical study involving one lingual carcinoma patient who was subjected to endoarterial therapy using ^{211}At-labeled HSA microspheres [84]. While complete remission was achieved, except for a slight depression in thyroid function, no adverse effects were observed. The feasibility of using silver nanoparticles covalently coated with polyethylene oxide as a carrier for ^{211}At also has been investigated [85]. Quantitative labeling yields have been obtained under reducing conditions and the labeled particles were stable even when chased with a large excess of chloride ions. Hartman *et al.* [86] have developed ultra short single walled carbon nanotubes (US-SWNT) loaded with ^{211}AtCl, which was retained by noncovalent van der Waals interactions within the interior side walls of the nanotubes [86]. Reasonable stability with respect to retention of ^{211}At activity was achieved after a serum challenge. Both silver nanoparticles and US-SWNT are amenable to modification with tumor targeting vectors. Liposomes are sequestered by tumors by the enhanced permeability and retention effect and possible tumor delivery of ^{211}At by conjugating astatinated molecules to liposomes has been proposed [87].

Astatinated Naphthaquinone and Methylene Blue Derivatives

The alkaline phosphatase isozyme, onco-APase is over expressed by certain epithelial and germ cell tumors and is a target for several 1,4-naphthoquinone diphosphates. As we reported in our earlier review [12], Brown and colleagues have synthesized astatinated naphthoquinone derivatives as a means to selectively deliver ^{211}At to tumor. Since that review, no further work on this topic has appeared. Melanoma is a radioresistant cancer and for this reason, targeted α-particle therapy should be beneficial for its treatment. The pheothiazin dye methylene blue (MB) has a very high affinity for melanin, which is synthesized at elevated levels by pigmented melanoma. Brown, Link and colleagues have investigated the usefulness of astatinated methylene blue for the treatment of melanoma (Summarized in Reference [12]). The group from Dubna also has evaluated methylene blue labeled with ^{211}At in preclinical models [88, 89]. They found that the [^{211}At]MB accumulation rate in pigmented melanoma cells *in vitro* was two times higher than that in non-pigmented cells [88]. The therapeutic effectiveness of [^{211}At]MB in pigmented melanoma cells was an order of magnitude higher than in normal fibroblasts. The tumor uptake *in vivo* of [^{131}I]MB reached a maximum of 5% at 5 h after i.v. administration and retained at the same level within 24 h thereafter; the pharmacokinetics of [^{211}At]MB was similar to that of [^{131}I]MB.

Agents that Undergo DNA Incorporation

Targeting DNA is the most effective way of inflicting cell kills by ionizing radiation; thus, localizing the radionuclide in close proximity to DNA or, even better, getting it incorporated in the DNA should be ideal. This is especially critical for those radionuclides such as ^{125}I that emit very short range Auger and Cöster-Kronig electrons. Extreme cytotoxicity for cells undergoing DNA synthesis has been demonstrated with the thymidine analogue, 5-iodo-2′-deoxyuridine (IUdR) labeled with ^{125}I and ^{123}I. However, the strength of this agent, its specificity for rapidly dividing cells, is also its most severe drawback in that tumor cells not undergoing DNA synthesis during their exposure to this agent will not be sensitive to its cytotoxic effects. It was hypothesized that an analogue of IUdR labeled with ^{211}At will be cytotoxic not only to cells which incorporate the α-particle-emitting agent into its DNA *via* the high LET α-particle recoil nuclei but also to adjacent cells due to its emission of relatively longer range α-particles. The astatinated analogue, 5-[^{211}At]astato-2′-deoxyuridine (AUdR; Fig. **3**) was first synthesized by Roessler *et al.* [90] from an amino precursor *via* a diazonium salt. The radiochemical yield was a meager 3% and the labeled AUdR was contaminated with other byproducts. Subsequently, it was synthesized from a mercury precursor; although higher yields were obtained, it was necessary to use carrier iodide in the reaction [52]. We developed a method for the synthesis of AUdR at a no-carrier-added level from a tin precursor in excellent radiochemical yields [91]; this method was adapted by other investigators subsequently [92, 93]. Substitution of ^{211}At for iodine in IUdR did not compromise its biological characteristics; the uptake of AUdR in D-247 MG human glioma and SK-Mel-28 human melanoma cells was nearly identical to that of IUdR and increased linearly with radioactivity concentration; furthermore, the uptake of both of these radiopharmaceuticals was abrogated by 10 μM IUdR [91]. AUdR was demonstrated to be extremely cytotoxic to these cells as reduction in survival to 37% was achieved with only 1-3 ^{211}At atoms bound per cell [91,94]. Using the neutral elution method, the yield for DNA double strand breaks was shown to be 10-fold higher for [^{211}At]AUdR compared to that for [^{125}I]IUdR [95].

Despite these encouraging results, AUdR may not be suitable as an endoradiotherapeutic agent if it has to be administered intravenously due to its poor stability. IUdR is known to undergo rapid deiodination *in vivo* and is also subject to degradation by nucleoside phosphorylases. Because the carbon-astatine bond is weaker than the carbon-iodine bond, AUdR is expected to behave similarly if not worse. Substitution of 2′-hydrogen in nucleosides with the hydrogen bioisostere fluorine is a tactic that is employed to bring about increased *in vivo* stability to these molecules without sacrificing their biological characteristics. A fluorine substituted analogue of IUdR, 5-iodo-1-(2-deoxy-2-fluoro-β-D-arabinofuranosyl)uracil (FIAU) has been developed and shown to be a stable alternative to IUdR. We have developed a method for the no-carrier-added synthesis of FIAU from a tin precursor, and by using this tin precursor, synthesized the astatinated analogue, 5-[^{211}At]astato-1-(2-deoxy-2-fluoro-β-D-arabinofuranosyl)uracil (FAAU; Fig. **3**) [96]. While the uptake of [^{125}I]FIAU in D-247 MG human glioma cells *in vitro* was 20-fold higher than that of [^{125}I]IUdR, a similarly enhanced uptake was not seen for FAAU over AUdR. While the fluorine substitution increased the stability of AUdR with respect to the glycosidic bond cleavage, extensive deastatination was still a problem. These results suggest that therapeutic applications of AUdR and FAAU may be limited to settings where they can be administered by non-intravenous routes.

Meta-[^{211}At]Astatobenzylguanidine

Meta-iodobenzylguanidine (MIBG) is a functional analogue of the neurotransmitter norepinephrine and is sequestered into the cells of sympathomedullary tissues by the norepinephrine transporter (NET). Because a number of neuroendocrine tumors such as neuroblastoma over express NET, radiolabeled MIBG has been used extensively in the diagnosis and treatment of these cancers. While radioiodinated MIBG has excelled as an

imaging agent, the therapeutic efficacy of [^{131}I]MIBG, especially in the case of neuroblastoma, is not that impressive. One of the contributing factors for this lackluster performance is related to the physical properties of the ^{131}I. Neuroblastoma is known to undergo metastases and as described before long range β-particles that are emitted by ^{131}I are not ideal for the treatment of micrometastatic diseases. Hypothesizing that an astatinated analogue of MIBG will be an excellent candidate for the treatment of such smaller tumors, we developed a method for the synthesis of *meta*-[^{211}At]astatobenzylguanidine (MABG; Fig. **4**) at high specific activities (16,000 TBq/mmol) [53]. Our earlier attempts to synthesize a tin precursor from which MABG could be synthesized in a single step were futile and we resorted to a silicon precursor; however, recently we were able to synthesize the elusive tin precursor in a protected form and demonstrated its usefulness for the synthesis of various radioiodinated MIBG and MABG [54]. Further, by utilizing a tin precursor that was anchored to a solid support, MABG was synthesized by a kit method in a sufficient quantity and quality suitable for clinical evaluations [97].

Utilizing SK-N-SH human neuroblastoma cells, it has been demonstrated that MABG is analogous to MIBG [53,98]. Its uptake in these cells was similar to that of MIBG and was blocked by agents and conditions that inhibit NET suggesting that substitution of iodine in MIBG by ^{211}At did not compromise the biological characteristics of the compound. The ability of SK-N-SH cells to retain MABG, after an initial uptake, also was similar to that of [^{131}I] MIBG. Paired-label biodistribution of [^{131}I]MIBG and MABG in normal mice indicated striking similarity in organ levels for the two agents especially in thyroid, spleen and lungs [53]. Because spleen and lungs have remarkable avidity for astatide, the similar uptake of ^{131}I and ^{211}At suggest that MABG is quite stable to deastatination *in vivo*. MABG was evaluated in athymic mice bearing subcutaneous SK-N-SH xenografts also [99]. Statistically significant higher uptake of MABG, compared to that of co-administered [^{131}I]MIBG, was seen in tumor tissue and this uptake was reduced to half with NET inhibitor desipramine. Like MIBG, MABG also demonstrated high myocardial uptake because heart is very rich with sympathetic neurons. Although no myocardial radiotoxicity has been reported from clinical administration of up to Curie (37 GBq) quantities of [^{131}I]MIBG, due to the high LET nature of the α-particles, this is an issue that needs to be considered before MABG can be administered intravenously in patients. Treatment with both unlabeled MIBG (4 mg/kg) and the vesicular uptake inhibitor tetrabenazine (20 mg/kg) reduced the uptake of MABG in heart without concomitant reduction in tumor suggesting that these are approaches that can be used to reduce any potential myocardial toxicity of MABG.

The superior cytotoxicity that MABG can deliver, compared to [^{131}I]MIBG, was demonstrated in a number of experiments. The ability of SK-N-SH cells to incorporate [^{3}H]thymidine was reduced to less than 50% of control values when treated with 118 Bq of MABG whereas no significant reduction in [^{3}H]thymidine uptake was seen when the cells were treated with up to 2960 Bq of no-carrier-added (n.c.a.) [^{131}I]MIBG under the same conditions [98]. From clonogenic assays using SK-N-SH cells, D_0 values of 0.215 kBq/ml and 3.84×10^2 kBq/ml were obtained for MABG and n.c.a. [^{131}I]MIBG, respectively suggesting that, under single cell conditions, the α-particle emitter is more than 1000-fold more cytotoxic [100]. Further, the cytotoxicity of MABG was 80-fold higher than that obtained for [^{211}At]astatide, confirming a significant advantage for targeted versus nonspecific α-particle irradiation. The D_0 values for MABG in two other NET-expressing neuroblastoma cells were equivalent to 6-7 bound atoms/cell and were similar to that obtained for SK-N-SH cells [100]; similar values have been obtained for two medulloblastoma cell lines [101]. The exquisite toxicity of MABG compared with that of Auger electron emitting [$^{123/125}$I]MIBG and β-particle emitting [^{131}I]MIBG, has been demonstrated in small human neuroblastoma multicellular spheroids as well [102].

Targeting of non NET-expressing tumor cells with MABG *via* a gene therapy approach also has been explored. Using human telom-erase promoters, which are more specific for tumor than normal tissues, high levels of NET expression was induced in UVW glioma cells [103]. The toxicity of [^{131}I]MIBG or MABG to the wild type UVW glioma cells and those transfected with the NET gene under the control of RSV, and the telomerase promoters hTR or hTERT was determined in multicellular mosaic spheroids. Little reduction in surviving fraction was observed in spheroids composed of non transfected UVW cells on treatment with either of the radiopharmaceuticals, suggesting that expression of functional NET is needed for cell kill using these radiolabeled NET substrates in these radioresistant glioma cells. On the other hand, all NET expressing spheroids regardless of the promoter driving NET expression succumbed to [^{131}I]MIBG-mediated cell kill in a dose dependent manner. With MABG, the dose required to reduce survival to 0.1% (log SF = 0.001) was roughly similar for all three transfectants, suggesting that a similar dose of MABG resulted in equivalent cell kill regardless of the strength of the promoter driving NET gene expression. As expected from the exquisite toxicity of MABG, the radioactivity levels required were 400-1000-fold lower than those required when [^{131}I]MIBG was used as the therapeutic. It has been demonstrated that MIBG derivatives labeled with α-, β-, and Auger electron-emitting radionuclides can elicit radiation induced biological bystander effect (RIBBE), which helps to sterilize those cells in which the NET gene is under expressed or not expressed [104]. Thus, the lack of efficacy of MABG due to the shorter range of alpha particles may be overcome by the substantial RIBBE that it generates. An accompanying article in this issue by Mairs *et al.* has dwelt at length the various aspects of this research. This group also has investigated the use of intracellularly concentrated MABG for inducing wild-type p53 activated fragment (WAF^{1}), a cyclin-dependent kinase inhibitor, for promoting transgene expression [105].

For use in positron emission tomographic imaging, a fluorine-substitued analogue of MIBG that can be labeled with the positron emitter ^{18}F has been developed. This derivative, 4-[^{18}F] fluoro-3-iodobenzylguanidine ([^{18}F]FIBG) was shown to be a useful positron emitter analogue of MIBG. Subsequently, FIBG was labeled with both ^{131}I and ^{211}At and these compounds were shown to have biological characteristics similar to that of MIBG [106]. The astatinated analogue, 3-[^{211}At]astato-4-fluorobenzylguanidine ([^{211}At]AFBG) demonstrated a significantly higher retention in SK-N-SH human neuroblastoma cells *in vitro* compared to MABG [107]. This suggests that a higher cumulative radiation dose can be delivered to the tumor with the fluorine substituted analogue; however, the uptake of FABG in normal tissues in mice was higher indicating that it may not have any particular advantage over MABG in the targeted α-particle therapy, at least for intravenous applications.

Biotin Derivatives

The large size of mAbs is disadvantageous in their use in radio-immunotherapy (RIT) in tandem with short lived radionuclides such as ^{211}At. A strategy that is often used to maximize the tumor delivery of radiation dose in RIT is pretargeting. In pretargeting, the unlabeled mAb conjugate is administered first and is allowed to localize in the tumor and clear from the circulation. After an appropriate time, when a maximal tumor to background ratio can be achieved, a small molecule labeled with the desired radionuclide and that has affinity to the mAb conjugate is administered. In the most commonly used pretargeting strategy, the high affinity ($10^{13} – 10^{15}$ M^{-1}) of the egg white protein avidin (65 kDa) or its bacterial analogue streptavidin (54 kDa) to the vitamin H, D-biotin (244 Da) is exploited to achieve this binding interaction.

The synthesis and evaluation of three biotin derivatives labeled with ^{211}At have been described and we have covered this in our previous review [12]. To improve pharmacokinetics, the development of charge-modified polylysine derivatives of different molecular weights

decorated with astatinated biotin as effector molecules for pretargeted therapy of intraperitoneal tumors has been reported [108]. When the molecular weight of the polylysine was about 13 kDa, rapid clearance *via* the kidneys was observed after i.p. administration in tumor-free mice. Higher molecular weight constructs demonstrated higher liver uptake and, as a result of this, higher dehalogenation. Subsequently, this group of investigators compared the tissue distribution of poly-D-lysine versus that of poly-L-lysine [109]. Because there was higher cumulative kidney uptake of the D-than the L-isoform, presumably due to the faster decomposition of the latter, the authors suggest that the use of ^{211}At-labeled L-isomer may yield higher therapeutic efficacy. Wilbur *et al*. reported the synthesis and evaluation of a number of astatinated aryl- and *nido*-carboranyl-biotin derivatives [110]. The presence of a COOH group in the α-position of the biotinamide moiety imparted stability toward biotinamidase without sacrificing avidin binding ability. The derivatives containing a *nido*-carborane moiety were more inert to *in vivo* deastatination. However, even after introducing a trialky-lamine function to counter unwanted putative interaction with the surface cationic charges of serum proteins, these derivatives had a long retention in blood which may defeat the very purpose of pre-targeting. Obviously, further work is needed before ^{211}At-labeled biotin derivatives reach the stage where clinical evaluation is warranted.

Bisphosphonates

Bony metastases often result from lung, breast and prostate cancers in their advanced stage. To alleviate the pain and to prevent tumor progression of such metastases, bone seeking bisphosphonate complexes labeled with various β-emitting radiopharmaceuticals have been developed. Because of the potential for irradiating bone marrow by the long range β-particles from these agents, analogues labeled with α-particle emitters are desired. Our group has developed methods for labeling Pamidronate®, a commercially available bis-phosphonate, with ^{211}At [111]. Astatine-211 labeled templates *N*-succinimidyl 3-[^{211}At]astatobenzoate (SAB) and *N*-succinimidyl 5-[^{211}At]astatopyridine-3-carboxylate (SAPC) were first synthesized and then conjugated to 3-amino-1-hydroxypropylidene-1,1-bisphosphonate to render 1-(3-[^{211}At]astato)benzamido-3-hydroxypropylidene-3,3-bisphosphonate ([^{211}At]ABPB) and 1-(5-[^{211}At]-astato-pyridine-3-carboxamido-3-hydroxypropylidene-3,3-bisphosphonate ([^{211}At]APPB) in 60-80% yield. HPLC analysis indicated that both labeled bisphosphonates are stable in murine and human serum *in vitro* over a period of 24 h. Both compounds demonstrated high bone uptake (35–47% ID/g) in normal mice and co- or pre-injection of Pamidronate® reduced the uptake in normal tissues without concomitant decrease in bone uptake [112]. Dosimetric estimates showed that bone surface to bone marrow dose ratios were 3 times higher for the astatinated analogues than for ^{131}I-labeled congeners [113] suggesting that it may be advantageous to use the α-particle emitting analogues for the treatment of osseous cancers.

Benzamides for Targeting Melanoma

Several tumors including melanoma and glioma are known to over express σ_2 receptors and benzamides accumulate in these tumors, presumably mediated by their binding to σ_2 receptors. Based on the high tumor accumulation and favorable pharmacokinetics of *N*-(2-piperidinylethyl) 4-[^{125}I]iodobenzamide ([^{125}I]IPAB), its astatinated analogue *N*-(2-piperidinylethyl) 4-[^{211}At]astatobenzamide ([^{211}At]APAB) was synthesized in 69–82% radiochemical yields from a tin precursor [114]. Compared to the radioiodinated analogue, a 2- to 3-fold higher binding of [^{211}At]APAB to SK-MEL 28 melanoma cells *in vitro* was seen. From a paired label biodistribution study of [^{211}At]APAB and [^{131}I]IPAB in normal mice, the accumulation of ^{211}At was shown to be substantially higher in lungs, stomach and spleen compared with that of ^{131}I suggesting that [^{211}At]APAB has undergone extensive deastatination *in vivo* and thus may not be suitable for intravenous administration. The n.c.a. synthesis of *N*-(2-diethylaminoethyl)-3-[^{211}At]astato-4-methoxybenzamide ([^{211}At]AMBA),

another potential agent for the alpha therapy of melanoma has been described but no studies on its evaluation have been reported [115].

Steroids

Steroid hormone receptors are over expressed by breast, prostate and ovarian cancers and the potential of targeting these tumors with radiolabeled steroids has been explored. For possible α-particle therapy of such cancers, attempts have been made to radiolabel steroids with ^{211}At. Visser *et al*. synthesized astatinated estradiol and cholesterol in a carrier-added form from their mercury precursors [52]. Estradiol derivatives containing ^{211}At on a vinylic carbon also have been synthesized at a no-carrier-added level from tin precursors [38,39]. The synthesis of 6-[^{211}At]astatomethyl-19-norcholest-5(10)-en-3β-ol, a potential agent presumed to target adrenal neoplasms, by the crown ether-mediated exchange halogenation has been reported [116]. High accumulation (136 – 181% ID/g) in adrenal glands in normal mice was seen; however, it underwent extensive deastatination *in vivo*.

PEPTIDES AND SMALL MOLECULAR WEIGHT PROTEINS

Peptides

Because of their favorable pharmacokinetics, low antigenicity and ease of synthesis, peptide radiopharmaceuticals play a significant role in nuclear medicine. There are a variety of bioactive peptides that can be targeted to a number of different receptors. Perhaps the most widely used class of peptides is the one that targets somatostatin receptors (SSTR), which are expressed by a number of cancers. The biological half lives of oligopeptides are ideally matched with the physical half life of ^{211}At and therefore astatinated peptides should be potentially useful in the targeted alpha therapy of cancer.

Oligopeptides are amenable for direct radioiodination provided they possess one or more tyrosine residues in their structure. However, due to the lability of iodotyrosine for *in vivo* dehalogenation, it is desirable that the radioiodine resides on a different moiety. Furthermore, it may be not be practical to astatinate peptides on their tyrosine residues due to the extreme instability of astatotyrosine. Peptides have been radioiodinated by conjugation with preformed labeled prosthetic groups such as *N*-succinimidyl 3-[*I]-iodobenzoate and *N*-succinimidyl 5-[*I]iodopyridine-3-carboxylate (SIPC). We have labeled the SSTR2-reactive octapeptide octreotide with ^{211}At using this strategy [117]. To prevent modification of the pharmacologically relevant lysine side chain, it was necessary to first protect it and subsequently remove the protecting group after conjugation. This necessitated the use of 3 HPLC purification steps, which in combination with the shorter half life of ^{211}At, reduced the effective over all radiochemical yields. To overcome this, the peptide was first conjugated with tin moiety; however, it still involved two radiochemical steps. To our knowledge, this is the first time a peptide has been modified with a tin function and subsequently radiohalogenated (Fig. **5**).

Subsequently, a better analogue of octreotide, octreotate was astatinated in a single step (Fig. **6**) [118]. The peptide was synthesized with an orthogonal protecting group on the lysine side chain and the *N*-terminal amino group was conjugated to a prosthetic group containing both a guanidine function and a tin moiety. The orthogonal protecting group was then removed, rendering the tin precursor peptide. Astatodestannylation and concomitant removal of Boc protecting groups on the guanidine function were achieved in a single step by the treatment of this tin precursor with ^{211}At and *tert*-butyl hydroperoxide in acetic acid at 70°C; however, typical radiochemical yields for astatination were only 15-20%. The astatinated peptide was taken up and internalized by the SSTR2-expressing D341 human medulloblastoma cells *in vitro* to the same degree as that seen for the same peptide radioiodinated with the analogous

prosthetic group (Fig. **7**). These results demonstrate that octreotate can be labeled with ^{211}At using this strategy without sacrificing the SSTR2 binding ability of the peptide.

The ability to synthesize another ^{211}At-labeled octreotate analogue from a tin precursor in a single step has been demonstrated (Fig. **8**) [55]. The attachment of a sugar residue to the *N*-terminus of octreotide or octreotate has been shown to improve receptor binding affinity and tumor and normal organ pharmacokinetics of these peptides. To accommodate both the prosthetic group and the sugar residue in order to combine these strategies, an extra lysine (lys^0) was attached to the *N*-terminus of octreotate. Then a fructose unit was attached to the α-amino group and a 3-(trimethylstannyl) benzoyl group to the ε-amino group of lys^0, after which the orthogonal protecting group on lys^5 was removed to obtain the tin precursor. Astatodemetallation of this precursor peptide gave the ^{211}At-labeled peptide in about 50% radiochemical yield. While the affinity to SSTR2 did not seem to be affected by this modification as demonstrated from receptor binding assay of the cognate iodinated peptide, both the radioiodinated and astatinated peptides had a lower uptake and internalization in D341 cells *in vitro* compared to a gold standard octreotate derivative. Although methods have been developed for the astatination of octreotate derivatives that can possibly be applied to other peptides as well, other modifications may be necessary to improve specific tumor targeting of these labeled peptides.

Small Proteins/Large Peptides

With the goal of treating hepatocarcinoma and other insulin receptor expressing cancers, 5.8 kDa insulin has been labeled with ^{211}At using preformed *N*-succinimidyl 5-[^{211}At] astatopyridine-3-carboxylate (SAPC) in conjugation yields of 30-40% [119]. The labeled product was stable in PBS at room temperature up to 24 h. Similar stability was imputed *in vivo* also based on the fact that the uptake of labeled insulin at 30 min and 3 h in lung, spleen and stomach in normal mice was 15- to 20-fold lower than that of free astatide.

Affibody molecules, proteins of molecular weight 6-7 kDa, are derived from one of the IgG binding domains of staphylococcal protein A by phage display methods [120,121]. The relatively small size allows their synthesis by chemical means with homogeneous site-specific introduction of prosthetic groups amenable for radiolabeling. Indeed, affibodies have been labeled with various radionuclides including ^{99m}Tc, ^{111}In, ^{177}Lu and ^{90}Y. Two affibody molecules, $(Z_{HER2:4})_2$ and $Z_{HER2:342}$-cys were recently labeled with ^{211}At using *N*-succinimidyl 4-[^{211}At]astatobenzoate (PAB); $Z_{ZHER2:342}$-cys was also conjugated with the ^{211}At-labeled B10 decaborate prosthetic group containing a maleimide function [122]. In tumor-bearing mice, the uptake of ^{211}At from both constructs labeled using PAB was substantially higher in lungs, stomach, and thyroid compared to the ^{125}I uptake from the corresponding ^{125}I-labeled constructs. The uptake in some normal tissues could be reduced by preadministration of lysine or sodium thiocyanate. The uptake of ^{211}At from ZHER2:342-cys labeled with the B10 template in lungs, thyroid and stomach was considerably less; however, there was a concomitant increase in hepatic and renal uptake. The authors concluded that although the pharmacokinetics of affibody molecules are ideal for labeling with ^{211}At the labeling chemistry needs to be improved before this strategy can be translated to clinical studies.

To target epidermal growth factor receptor (EGFR), which is expressed by a number of cancers, human EGF (~6.2 kDa) has been labeled with ^{211}At. To label the protein in a stable manner, the use of *nido*-carborane prosthetic group was employed [123]. EGF was first derivatized with 7-(3-amino-propyl)-7,8-dicarba-*nido*-undecaborate (−) (ANC-1) using either glutaraldehye (EGF-GA-ANC) or the bifunctional cross linking agent, sulfo-MBS; in the latter case, EGF was first treated with Traut's reagent to generate sulfhydryl groups (EGF-TR-ANC). EGF conjugated with ANC-1 by both methods was astatinated directly using Chloramine-T as the

oxidizing agent. For comparison, EGF was also astatinated using the PAB reagent. Highest radiochemical yields (68 ± 9%) were obtained for the direct astatination of EGF-ANC-1 conjugate derived using glutaraldehyde. In comparison, 32 ± 18%, 44 ± 5%, and 5 ± 7% yields were obtained for EGF-TR-ANC, EGF-PAB, and unmodified EGF (direct labeling), respectively. The *in vitro* stability of both EGF-GA-ANC and EGF-PAB were similar with 88.1 ± 1.5% and 81.6 ± 1.4%, respectively, of the astatine associated with intact peptide after 15 h of incubation in PBS. Because gefitinib, an EGFR tyrosine kinase inhibitor, has been shown to enhance the antitumor effect of ionizing radiation, its effect on the uptake of ^{211}At-labeled EGF in EGFR-expressing glioma cells was studied [124,125]. In comparison with untreated cells, treatment with 1 μM gefitinib resulted in 3.5-fold increase in the uptake EGF labeled with ^{211}At using PAB in U343 glioma cells. Further, this difference persisted over a 21 h (3 half lives of ^{211}At) incubation period and excess of unlabeled EGF blocked the uptake significantly in both cases. There was a concomitant reduction (3.5-fold) in survival of gefitinib-resistant U343 cells treated with both ^{211}At-labeled EGF and gefitinib compared to that treated with ^{211}At-labeled EGF alone. Paradoxically, ^{211}At-labeled EGF treatment resulted in low survival of gefitinib-sensitive A431 squamous carcinoma cells but co-treatment with gefitinib increased the survival by 20-fold. These results were interpreted as suggesting that combined treatment with gefitinib might increase the effect of ligand-mediated radionuclide therapy in gefitinib-resistant tumors and decrease the effect of such therapy in gefitinib-sensitive tumors. In another study, the effect of lysosomotropic agents such as ammonium chloride and chloroquine on the uptake, retention and cytotoxicity of ^{211}At-labeled EGF in A431 cells was investigated [126]. About a 2-fold increase in uptake and retention of ^{211}At-labeled EGF by these cells was seen when they were treated with 20 mM ammonium chloride. A radiation dose corresponding to 191 decays per cell was calculated for cells treated with ammonium chloride compared to 112 decays per cell for the group that was not treated with the lysosomotropic agent. The delay in the growth of cells treated with ^{211}At-labeled EGF or ammonium chloride alone or in combination was compared to untreated controls. Treatment with ammonium chloride alone did not cause any growth delay nor was there any significant reduction in the survival of cells in which the uptake of ^{211}At-labeled EGF was blocked by treatment with excess unlabeled EGF suggesting no significant effect from radioactivity in the medium. There was a significant ($p < 0.001$) delay in growth (24 ± 5 days) for cells treated with ^{211}At-labeled EGF and no regrowth was seen when ^{211}At-labeled EGF was combined with ammonium chloride. Provided the administration of lysosomotropic agents does not cause undue toxicity, use of these agents may increase therapeutic efficacy of ^{211}At-EGF. In yet another study, the uptake, retention and intracellular processing of ^{211}At-labeled EGF was compared with that of its radioiodinated analogue in A431 cells [127]. The extent of uptake, retention and internalized radioactivity was significantly higher in the case of the astatinated derivative. The authors have speculated that this might be due to higher rate of dehalogenation of the astato analogue and possible binding of free astatine to cellular proteins.

ANTIBODIES AND THEIR ENGINEERED FRAGMENTS

Due to the slow clearance of IgG molecules from the blood, ^{211}At-labeled intact mAbs may be best suited to settings where the labeled mAb can be administered loco-regionally. On the other hand, ^{211}At-labeled small molecular weight mAb fragments may find application for systemic administration because of their lower molecular weight. In the following sections, the approaches for labeling mAbs and their fragments as well as the *in vitro* and *in vivo* evaluation of these labeled molecules including a clinical trial will be described.

Chemistry

While a very large number of proteins and antibodies have been radioiodinated by the direct electrophilic method, which incorporates the radioiodine at the *ortho* position of the phenolic

hydroxyl group of tyrosine moieties, this strategy for astatination has been found to be futile due to the extreme instability of astatotyrosine [48,128]. As an alternative, the possibility of introducing the astatine onto histidine residues in proteins has been explored [129]. While the authors were able to astatinate several imidazole derivatives from mercury precursors, they were found to be unstable under the oxidizing conditions needed for protein labeling. This necessitated the development of conjugation labeling methods and one of the first methods developed was labeling proteins by reacting with preformed [^{211}At]astatobenzoic acid, which was derived from a diazonium precursor [130-133]. The labeled acid was activated by converting it to the isobutyrl anhydride derivative and coupled subsequently to the protein. This method was not found to be generally very attractive because of the modest radiochemical yields and formation of several undesirable byproducts. However, successful labeling of a mAb and its Fab fragment utilizing this method has been reported by other investigators [134,135].

Subsequently, several labeled active esters that can be derived from suitable precursors and that can be conjugated to proteins under mild conditions in good yields with the preservation of protein function, have been developed. Although conjugation agents that are reactive with amine, sulfhydryl, and carbohydrate functions have been developed for the radiohalogenation of proteins, astatination has been performed predominantly using active esters which mainly react with amine moieties. *N*-succinimidyl 3-[^{211}At]astatobenzoate (SAB) was the first such agent developed and was derived from a tin precursor, *N*-succinimidyl 3-(tri-*n*-butylstannyl) benzoate [136]. An isomeric agent, *N*-succinimidyl 4-[^{211}At]astatobenzoate (PAB) also has been synthesized in a similar manner [137] and both these reagents have been used for labeling a variety of different proteins [138-145].

A number of other ^{211}At-labeled succinimidyl esters have been reported ever since. Hypothesizing that reduction in dehalogenation would be achieved by introducing substituents on both *ortho* positions of the halogen carrying carbon, a dimethoxy derivative of SAB has been developed [146]. This agent could be derived from either a trimethylstannyl or a tributylstannyl precursor in similar radiochemical yields. Biodistribution of a mAb F(ab')$_2$ fragment labeled with this agent indicated normal tissue uptake at early time points similar to that of the radioiodinated congener but by 14.5 h, substantially higher uptake of ^{211}At in spleen, lungs and stomach were seen. The synthesis and evaluation of analogues of SAB and PAB with other substituents in the benzene ring as well as that of *N*-succinimidyl 4-[^{211}At] astatophenethyl succinimate (SAPS) and its *N*-methyl analogue (Methyl-SAPS) also have been reported [56,147,148]. The authors concluded that SAPS is a better agent than the benzoic acid derivatives with respect to labeling chemistry, blood clearance and normal tissue uptake. Methyl-SAPS was developed to obviate the inconsistencies in the radiolabeling and conjugation chemistry, and Herceptin labeled with Methyl-SAPS was found to be superior to that labeled with simple SAPS.

Hypothesizing that the degree of recognition of iodinated heterocyles by endogenous deiodinases may be less than that of carbocyclic analogues and therefore iodo-heterocycles may be more inert to *in vivo* deiodination, a radioiodination agent containing a pyridine ring in place of benzene ring was developed. In addition to being inert to deiodination, labeled catabolites resulting from proteins radioiodinated using this agent were expected to clear faster from normal tissues due to their lower lipophilicity. Further, use of this agent to label mAbs that undergo internalization after receptor binding should result in a higher tumor-associated radioactivity, compared to the same mAb radioiodinated with the carbocyclic analogue, due to the fact that the catabolites will be protonated at lysosomal pH thereby preventing their traversal across lysosomal membranes. For these reasons, the astatinated analogue of this agen t, *N*-succinimidyl 5-[^{211}At]astato-pyridine-3-carboxylate (SAPC) was synthesized and evaluated [149]. SAPC was synthesized from a tin precursor in about 50% radiochemical yields and coupled to L8A4, an anti-EGFRvIII mAb in 46% conjugation efficiency. The affinity and

immunoreactive fraction of the astatinated mAb was similar to that of the mAb radioiodinated using the same template. Also, the internalization and catabolism *in vitro* and the biodistribution *in vivo* of the two labeled mAbs were similar, suggesting the potential usefulness of the SAPC reagent for labeling internalizing mAbs.

Because guanidines have a pKa of about 13, they are expected to remain exclusively protonated at lysosomal pH. It was hypothesized that catabolites resulting from proteins labeled with prosthetic groups containing guanidine function will be trapped within the tumor cells due to the presence of positively charged guanidine moiety. To investigate this, a radioiodination agent containing the guanidine group was developed. Indeed, when radioiodinated with *N*-succinimidyl 4-guanidinomethyl-3-[*I]iodobenzoate ([*I]SGMIB), radioactivity from mAbs that undergo internalization was retained to a substantially higher degree by tumor cells both *in vitro* and *in vivo*. To exploit the advantage of this template in targeted alpha particle therapy, the astatinated analogue *N*-succinimidyl 3-[^{211}At]- astato-4-guanidinomethylbenzoate (SAGMB) (Fig. **9**) was developed [150]. SAGMB was synthesized from the same tin precursor used for the preparation of [*I]SGMIB in 62% radiochemical yields and coupled to the anti-EGFRvIII mAb L8A4 in 36% yields. Paired-label *in vitro* internalization assays using U87MG·ΔEGFR glioma cells demonstrated that the cellular retention of L8A4 labeled with SAGMB was similar to that labeled with [^{131}I]SGMIB and was 3- to 4-fold higher than that seen for the directly radioiodinated L8A4 (Fig. **10**). Over a 24 h period, the tumor uptake *in vivo* was similar for L8A4 labeled with SAGMB and [^{131}I]SGMIB (Fig. **11**). The uptake of ^{211}At in tissues such as lung, spleen and stomach that sequester astatide was higher than that of ^{131}I; however, the ^{211}At /^{131}I ratios seen in these tissues were considerably lower than that seen with other labeling methods. Taken together, SAGMB may be a useful agent for labeling internalizing mAbs (and possibly low molecular weight mAb fragments) with ^{211}At.

As described in a previous section, to exploit the higher stability of boron-astatine bond strength, Wilbur's group has developed methods for labeling mAbs with ^{211}At using boron cage pendant groups [151]. Higher *in vivo* stability with respect to deastatination was obtained by using the so called Venus fly trap complexes; however, long blood residence times and high hepatic uptake was a problem [141]. A Fab' fragment conjugated with the anionic *closo*-decaborate-(2-) could be directly astatinated in 58-75% radiochemical yields and the labeled fragment demonstrated good *in vivo* stability [59]. However, uptake of the conjugate was higher in normal tissues, especially the liver, compared to that of unconjugated Fab' that was labeled with radioiodine (direct or PIB) or with ^{211}At (PAB). More details of these studies can be found in an accompanying article of this issue by Wilbur.

Another method for directly labeling proteins with ^{211}At utilized the metallic properties of astatine. In an early study, DTPA was first labeled with ^{211}At and the labeled complex was conjugated to a polyclonal antibody [152]. In another study, the IgG molecule was first derivatized with DTPA and then the DTPA-IgG conjugate was labeled with ^{211}At in 80 - 85% yields [62]. While the stability of thus labeled protein *in vitro* was reasonable, it was found to be very unstable *in vivo*.

In Vitro Cytotoxicity

In determining the cytotoxicity of ^{211}At-labeled mAbs, the geometric arrangement of target cells is an important factor that needs to be considered because of the short range of α-particles. The contribution to cell kill from unbound ^{211}At from the media and the cell-to-cell cross fire irradiation can vary considerably from one assay format to another. Various formats such as single cell suspension, monolayer, and multicellular spheroids have been utilized for studying the cytotoxicity of ^{211}At-labeled mAbs.

An anti-human leukocyte antibody, BK 19.45 and the plant lectin Conconavalin A (MW = 96 kDa) have been labeled with ^{211}At and their cytotoxicity determined [153]. Cell pellets containing 1-5 × 10^6 cells were treated with labeled proteins and the clonogenic potential of the treated cells was determined. With the antibody, the radiation dose needed to reduce survival to 37% (D_0) was determined to be 12 ^{211}At atoms per cell. The cytotoxic potential of TP3, a mAb that reacts with an antigen present on the osteosarcoma cells, was evaluated in 3 human osteosarcoma cells under single cell conditions [154]. Cell survival was determined after treatment of the cells with 1) ^{211}At-TP3 of three different specific activities (MBq/mg), 2) ^{211}At-labeled BSA, 3) free [^{211}At]astatide, and 4) external beam x-rays. The survival curves were similar for all cell lines subjected to 3 latter agents/conditions. On the other hand, the survival curves among the 3 cell lines differed significantly after treatment with ^{211}At-labeled TP3 and the difference was related to the degree of antigen expression. Additionally, survival of the cell lines was dependent on the specific radioactivity of the labeled mAb. Higher specific activity preparation demonstrated 80-fold higher potency compared to controls with a D_0 equivalent to 40 ^{211}At atoms bound per cell. The cytotoxicity of ^{211}At-TP3 also was determined using two osteosarcoma cell lines and one melanoma cell line in microcolonies consisting of 10-15 cells in planar arrays [155]. The therapeutic gain factors (TGF), calculated for survival levels, were in the range of 1.3 ± 0.4–4.5 ± 0.7 for ^{211}At-TP3 and was 1.6-fold higher in the case of the antigen-rich OHS cell line compared to that of the antigen-poor KPDX cell line. TGF values for free [^{211}At]astatide and ^{211}At-BSA were only 0.6 ± 0.1–1.0 ± 0.3. In yet another study, the cytotoxicity of ^{211}At-TP3 to OHS cells and to bone marrow cells was evaluated [156]. Cells in suspension were incubated with the labeled antibody and, after removal of unbound radioactivity, the survival was determined by a clonogenic assay. For comparison, the cells were also irradiated with a single dose of external γ-rays. The D_0 values estimated by microdosimetry after exposure to labeled mAb were 0.33 Gy and 1.1.8 Gy for OHS cells and bone marrow cells, respectively; these values after external γ-ray irradiation were 0.86 and 1.71 Gy.

The cytotoxicity of 2 ^{211}At-labeled mAbs, one reactive with the extracellular matrix antigen tenascin (81C6) and the other with the cell membrane antigen proteoglycan chondroitin sulfate (Mel-14) along with that of a nonspecific control mAb TPS 3.2 was evaluated in microcolonies of D-247 MG human glioma and SK-Mel-28 human melanoma cells [157]. The microcolonies of D-247 MG consisted of an average of 16 cells with a cell diameter of 18.5 μm and of SK-Mel-28 consisted of an average of 25 closely packed cells with a cell diameter of 20 μm. Cell uptake of ^{211}At increased linearly with labeled mAb concentration and, with a 18 kBq/ml concentration and a 1 h incubation, 2- to 5-times higher activity from the specific mAb was bound compared to control mAb. For both cell lines, achieving D_0 killing required an average of only 1-2 α-particle hits to the cell nucleus. Hypothesizing that hyperthermia may promote homogeneous tracer distribution, a sine qua non for α-particle therapy, the effect of hyperthermia on the cytotoxicity of ^{211}At-labeled 81C6 in D247-MG spheroids of radii greater than the maximum range of the α-particles was determined [158]. While the labeled mAb was effective in reducing the doubling time of the spheroids, hyperthermia did not have any significant effect on the uptake and distribution of the labeled mAb. The anti-CD20 mAb rituximab (aka IDEC-C2B8) was labeled with ^{211}At and the cell killing efficiency of the labeled mAb was determined by clonogenic assays in two B-lymphoma cell lines and in normal hematopoietic progenitor cells [159]. While the uptake of the labeled mAb increased as a function of initial radioactivity concentration in both control cells and antigen expressing RAEL cells, the uptake in the latter was about 15- to 20-fold higher. At an initial radioactivity concentration of 50 kBq/ml, the log cell kill value for RAEL cells were about 4-fold higher compared to control cells.

An anti-gastric cancer mAb and its Fab fragment were labeled with ^{211}At using 4-[^{211}At] astatobenzoic acid, which was prepared *via* a diazonium salt, and their toxicity *in vitro*

determined in M85 human gastric cancer cells along with that of free [^{211}At]astatide [134]. The labeled mAb and its fragment were about 2-fold more toxic than free [^{211}At]astatide. The possibility of treating disseminated ovarian cancer has been studied using a murine mAb labeled with ^{211}At [160-164]. This mAb, MOv18, recognizes a membrane folate-binding glycoprotein and reacts with 90% of human ovarian carcinomas. The labeled mAb bound to the ovarian cancer cells OVCAR-3 *in vitro* (about 5% of input radioactivity) only when the medium was devoid of folic acid. The ^{211}At-labeling of a chimeric mAb U36, reactive to tumor-associated antigen CD44v6 that is found on most human head and neck squamous cell carcinoma, and its evaluation has been reported [165]. The uptake, retention and internalization of the astatinated mAb by SSC-25 cells were similar to the same mAb labeled with radioiodine. Cells in monolayer were subjected to either unlabeled mAb or mAb labeled with ^{211}At and ^{131}I, and then clonogenic survival and cell growth assays were performed. While unlabeled mAb did not have any significant effect on the survival, there was a dose-dependent reduction in survival when the cells were treated with astatinated mAb. The survival was reduced to about 66% and 10% when the cells were incubated with astatinated mAb at doses equivalent to 12 and 50 decays per cell, respectively. The survival was reduced to only 85% when the cells were subjected to a dose equivalent to 50 decays per cell in the presence of a large excess of unlabeled mAb. When exposed to ^{131}I-labeled mAb at a dose equivalent to 55 decays per cell, 55% of the cells survived. Results obtained from cell growth assays were similar with that obtained from the clonogenic assay.

A slowly rotating, widely dispersed single cell suspension of Colo-205 human colorectal cancer cells was treated with ^{211}At-labeled C215 mAb and the cell survival was determined [166]. The number of ^{211}At decays per cell needed to reduce survival to 37% was calculated to be 35 ± 2. The cytotoxicity of ^{211}At-labeled trastuzumab, a mAb that reacts with HER2 receptors, was evaluated in three HER2-expressing breast cancer cells by clonogenic assays [167]. The specific radioactivity (kBq/μg) of the labeled mAb was shown to be an important factor in cell survival—the survival was inversely proportional to specific radioactivity. A pharmacokinetic model demonstrated that there was a competition between the labeled and unlabeled mAb. The survival curves were biphasic when the survival fractions were plotted against the radioactivity concentration but became mono-exponential after applying a pharmacokinetics/microdosimetry model to enable the results to be plotted vs. radiation dose. Compared to external beam therapy, the relative biological effectiveness of ^{211}At-labeled trastuzumab was about 10 times higher.

Evaluation in Animal Models

In a number of studies cited above as well as others, several ^{211}At-labeled mAbs or their engineered fragments have been evaluated in animals bearing tumor xenografts. Because it is the first ^{211}At-labeled targeted radiotherapeutic that was evaluated in cancer patients, the anti-tenascin mAb 81C6 will be described in a separate section. Probably the first ^{211}At-labeled mAb to be evaluated in tumor-bearing mice is the BK 19.9 antibody that has specificity for the human transferrin receptor [168,169]. A specific tumor localization, 2- to 5-fold higher than that seen for any other tissue, was obtained. A mAb (anti-thy 1.1, IgG1, OX7) labeled with ^{211}At was used in the treatment of mice bearing thy 1.1 T-cell lymphoma (A120) xenografts [170]. Forty-eight hours after receiving an i.v. injection of 10^3 or 10^5 A120 cells, mice were treated with phosphate-buffered saline, ^{211}At$^-$, antibody alone, or ^{211}At-OX7. Treatment with ^{211}At-OX7 increased the median survival time of mice compared to controls; at 200 days after treatment, 6 of the 15 mice given 10^5 cells and 21 of the 27 mice given 10^3 cells were alive. In the above two cases, the mAbs were labeled with ^{211}At using 4-[^{211}At] astatobenzoic acid derived from its diazonium salt precursor. An anti-gastric cancer mAb (3H11) and its Fab fragment also have been labeled this way and evaluated in mice bearing

M85 gastric cancer subcutaneous xenografts [134]. Counter-intuitively, the Fab fragment demonstrated a considerably higher tumor uptake than the intact mAb.

Our group has evaluated several mAbs and their fragments labeled with ^{211}At using *N*-succinimidyl 3-[^{211}At]astatobenzoate. The F(ab′)$_2$ fragment of Mel-14 (see above) was labeled with ^{211}At and its biodistribution over 24 h period compared in athymic mice bearing D-54 MG glioma xenografts to the same fragment radioiodinated with the same template [171]. The tumor retention of ^{211}At was essentially identical as that of ^{131}I except at 24 h. However, the labeled mAb underwent some deastatination as reflected by higher uptake of ^{211}At in spleen, lungs and stomach [172]. The effect of hyperthermia on the tumor uptake *in vivo* of this fragment has been investigated in another study [173]. Heating the tumors at 42 °C for 4 h resulted in a ~3-fold increase in the tumor uptake of ^{211}At-labeled Mel-14 F(ab′)$_2$. C110, a mAb against carcinoembrionic antigen and its F(ab′)$_2$ fragment were labeled with ^{211}At and ^{131}I and their biodistribution determined in normal mice [68]. While similar tissue distribution of the two nuclides was seen with the intact mAb, higher uptake of ^{211}At from the F(ab′)$_2$ fragment in spleen, lungs, and stomach was observed suggesting that astatinated fragment was less inert towards *in vivo* deastatination.

Over the years, several other mAbs and mAb fragments have been labeled with the astatobenzoate active ester agent and evaluated in animal models. Both the intact IgG and the Fab fragment of an antimelanoma mAb, NR-ML-05 were labeled with PAB and their biodistrubution, along with that of the radioiodinated counter-parts, was studied in athymic mice bearing A375 Met/Mix human tumor xenografts [174]. In the case of both proteins, the uptake in tumor tissues was similar for both isotopes over 22 h. The labeled intact mAb seemed to be stable with respect to deastatination because the uptake in spleen and lungs for the two isotopes were similar early; however, uptake of ^{211}At at later time points was considerably higher than that for ^{125}I. With the Fab fragment, the uptake of ^{211}At in all these three tissues was significantly higher at all time points suggesting considerable deastatination has taken place. The biodistribution of a ^{211}At-labeled F(ab′)$_2$ fragment of another mAb—anti-renal cell carcinoma antibody A6H—was evaluated in mice bearing TK-82 renal cell carcinoma xenografts [175]. The uptake of both astatinated and radioiodinated fragments in tumor, spleen and lungs were similar; however, higher retention of ^{211}At in the stomach was seen.

Targeted α-particle therapy is ideally suited for the treatment of ovarian cancers. The potential of ^{211}At-labeled mAb MOv18 for radioimmunotherapy has been investigated in nude mice with intraperitoneal ovarian cancer [160,164,176-178]. Intraperitoneal administration of the ^{211}At-labeled specific mAb was more effective than intravenous administration or the intraperitoneal administration of a ^{211}At-labeled nonspecific mAb. This group of investigators also has studied another mAb MX35 and its F(ab′)$_2$ fragment, labeled with ^{211}At using SAB, that are potentially useful for the treatment of ovarian carcinoma. MX35 is a murine IgG1 that reacts with a 95 kDa cell surface glycoprotein expressed by OVCAR-3 cells. The myelotoxicity of ^{211}At-MX35 (i.p. or i.v.) and its RBE, compared with that of the electron emitter ^{99m}Tc-MX35 and external beam irradiation, were determined in non-tumor-bearing nude mice [179]. A myelotoxic *in vivo* RBE of 3.4 ± 0.6 compared with ^{99m}Tc-MX35 and 5.0 ± 0.9 compared with external beam irradiation were obtained. In a subsequent study, the RBE of ^{211}At-MX35 F(ab′)$_2$ fragment was determined in tumor-bearing mice using growth inhibition as the end point [180]. Absorbed doses of 1.35, 2.65, and 3.70 Gy were delivered to the tumor after administering 0.33, 0.65, and 0.90 MBq, respectively of the labeled fragment. Compared to external beam irradiation, a RBE of 4.8 ± 0.7 was calculated for the ^{211}At irradiation. The therapeutic efficacy of ^{211}At-MX35 and its radiation absorbed dose were determined in athymic mice with intraperitoneally growing OVCAR-3 cells [164]. In 3 groups of animals treated (i.p.) with 400, 800, or 1200 kBq of ^{211}At-MX35, only 3 of 25 animals developed ascites. None of the animals had macroscopic tumors but 8 of them had microscopic

tumors. In comparison, in control groups either given saline or treated with unlabeled mAb, all of 18 animals had ascites and microscopic growth; 6 out 9 in each group had macroscopic tumors. The absorbed dose due to specific binding of ^{211}At-MX35 (400 kBq) for a cell cluster with a radius of 50 μm ranged from 413 to 223 Gy at distances of 0- and 45-μm from the cluster center. The therapeutic efficacy of ^{211}At-MX35 F(ab′)$_2$ fragment in comparison to that of a nonspecific fragment labeled with ^{211}At as a function of tumor size, has been determined by scanning electron microscopy [181,182]. When the tumor radii were ≤ 30 μm, the tumor-free fractions (TFF) resulting from the treatment with either mAb fragment were 95–100%. On the other hand, when the tumor sizes were larger, the specific mAb fragment yielded significant better TIFF. Another study investigated whether any therapeutic advantage can be obtained by fractionating the dose of ^{211}At-MX35 F(ab′)$_2$ fragment [183]. Animals were treated at 3 dose levels as a single injection or 3 equal fractions. While no particular therapeutic advantage was seen at any dose level by fractionating the dose, myelotoxicity was alleviated in the fractionated regimen. Treatment of radioresistant, HER2-expressing ovarian cancer in animal models with ^{211}At-labeled trastuzumab has been reported recently [184]. Several combinations of doses of labeled and unlabeled trastuzumab were administered. Therapeutic efficacy was dependent on both the mAb dose and the radioactivity dose with complete eradication of tumor when the mice were treated with the combination of 500 μg unlabeled mAb with 400 kBq of labeled mAb.

Several other mAbs, radiolabeled with ^{211}At using the astatobenzoyl template, have been evaluated in tumor models. Adult T-cell leukemia has an abundance of T cells, which express CD25 and mAbs 7G7/B6 and daclizumab react with different epitopes of CD25 (IL-2α). Treatment of a murine model of adult T-cell leukemia using ^{211}At-labeled mAb 7G7/B6 alone or in combination with daclizumab has been reported [185]. In NOD/SCID mice growing MET-1 human leukemia cells, administration of both ^{211}At-7G7/B6 (0.44 MBq) and daclizumab (100 μg) was more effective than either agent alone with 91% of the mice surviving for 94 days compared to a median survival of about 62 days in the control groups. Therapeutic efficacy of ^{211}At-7G7/B6 also was evaluated in NOD/SCID mice bearing karpas299 leukemia and in nude mice bearing SUDHL-1 lymphoma [186]. In the NOD/SCID mice model, the blood clearance and tissue distribution of ^{211}At-7G7/B6 was similar to that of ^{125}I-7G7/B6, and a Kaplan-Meier plot demonstrated significant prolongation in survival in the cohort treated with ^{211}At-7G7/B6 (0.56 MBq) compared to the saline control group and that treated with ^{211}At-labeled nonspecific mAb. In the solid tumor model (SUDHL-1), only a modest effect in inhibiting tumor cell growth *in vivo* was seen. Similarity in the biodistribution of ^{211}At and ^{125}I labeled rituximab, another anti-CD20 mAb, in non tumor-bearing mice has been demonstrated earlier [159]. An anti-CD30 mAb HeFi-1 also has been labeled with ^{211}At and its therapeutic effectiveness evaluated in the karpas299 model [187]. Treatment with ^{211}At-HeFi-1 (0.44 MBq) alone prolonged the survival of mice compared to those treated with unlabeled HeFi-1; the combination of labeled and unlabeled further increased survival.

To determine whether the tissue uptake data obtained from mAbs labeled with the positron emitters ^{76}Br and ^{124}I could be used to calculate the absorbed doses of the same mAb labeled with ^{211}At, A33—a mAb that reacts with an antigen present on most of colorectal cancers—was radiolabeled with ^{76}Br, ^{124}I, and ^{211}At using *N*-succinimidyl 4-halobenzoates and the biodistribution of the labeled mAbs was determined in Sprague Daley rats [188]. The absorbed doses to critical organs such as liver, kidney, bone, brain etc could be determined with 10% accuracy; however, it was necessary to use correction factors in determining doses to astatine-seeking organs such as stomach, spleen, and thyroid. A chimeric mAb U36 that recognizes CD44v6, a 200 kDa protein expressed by HNSCC cells, was labeled with ^{211}At and its therapeutic potential determined in mice bearing subcutaneous HNSCC xenografts [143]. Significant reduction in tumor growth was seen in groups treated with the labeled mAb, alone or in combination with unlabeled mAb; no undue toxicity was seen.

Evaluation of mAbs labeled with ^{211}At using other prosthetic groups also has been performed. The internalizing anti-EGFRvIII mAb L8A4 was astatinated with SAPC and its biodistribution was compared to that of the same mAb labeled with [^{131}I]SIPC in mice bearing U87MG·ΔEGFR glioma xenografts [149]. Except in stomach at all time points and in lungs, spleen, and thyroid at later time points, the uptake of ^{131}I and ^{211}At were similar over 24 h. L8A4 labeled with SAGMB has been evaluated in the above athymic mouse model along with the radioiodinated mAb [150]. Tumor uptake of both isotopes was identical over the 24 h period (Fig. **11**) and although the uptake of ^{211}At in astatine-avid tissues were higher compared to that of ^{131}I, the ^{211}At/^{131}I ratios in these tissues were considerably lower than that seen for other labeling methods.

Trastuzumab (Herceptin) was labeled with ^{211}At using three different *N*-succinimidyl esters and their biodistribution was studied in mice bearing LS-174T human colon adenocarcinoma xenografts [147]. Two of these templates, one with a methoxymethyl and the other with a methylthiomethyl groups ortho to the halogen-carrying carbon, were less advantageous compared to SAPS with respect to tumor uptake *in vivo*. SAPS was used to label a mAb (201B) that targets lung blood vessels [189]. Administration of 370 kBq of labeled mAb to mice bearing about 100 colonies of EMT-6 cells eradicated all lung tumors. While therapeutic effects, compared to control, also were achieved when ^{211}At-labeled glycine or nonspecific mAb were injected, the effective dose was roughly twice that of the specific mAb. Trastuzumab labeled with a *N*-methyl substituted derivative of SAPS also have been evaluated in LS-174T model and the methyl derivative was found to be slightly superior [56]. Therapeutic effectiveness of an anti-HER2 diabody C6.5 (~55 kDa) labeled with ^{211}At using the SAPS template in mice bearing HER2-positive MDA-MB-361/DYT2 xenografts has been demonstrated recently [190]. These investigators have shown that this diabody labeled with ^{90}Y and ^{131}I was suboptimal for the treatment of these mice. Hypothesizing that an α-emitter may be advantageous, they explored the therapeutic potential of this diabody labeled with ^{213}Bi; however, they found that the physical half-life of this radioisotope is too short to allow the localization of systemically administered therapeutic and hence resorted to ^{211}At. Indeed, a 30-day tumor growth delay was obtained with a single i.v. injection of 20 μCi of ^{211}At-SAPS-C6.5 diabody and a 57-day delay (60% tumor-free after 1 year) when a 45 μCi dose was used.

81C6: Preclinical Studies

Initial studies utilized the murine 81C6, an IgG_{2b} that reacts with an epitope present on fibronectin domains 11-12 of the tenascin molecule. The therapeutic effectiveness of ^{211}At-labeled murine 81C6 was determined in a rat model of neoplastic meningitis, which was created by intrathecal injection of TE-671 human rhabdomyosarcoma cells into an indwelling catheter inserted into the subarachnoid space [191]. Mice were treated with intrathecal injections of ^{211}At-81C6, saline or an ^{211}At-labeled nonspecific mAb. The nonspecific mAb (0.44 MBq) did not significantly increase survival compared with saline, while ^{211}At-81C6 at the same dose prolonged survival by 113% with 3 of 9 animals cured of their disease. Furthermore, 6 of 10 animals receiving 0.67 MBq ^{211}At-81C6 were alive after 300 days with no evidence of disease. The neuraxis from long term survivors was evaluated by histopathological analysis, and except for focal edema in one rat, no toxicities were seen. The lack of therapeutic effect observed with an ^{131}I-labeled mAb fragment in the same animal model is indicative of the potential advantage for using α-particle emitters in this setting.

To reduce immunogenicity, a human/mouse chimeric mAb was engineered and a paired-label comparison of the radioiodinated murine and the chimeric congeners demonstrated the superiority of the chimeric form with respect to *in vivo* stability and tumor uptake. Therefore, subsequent evaluations were carried out with the chimeric mAb. The tissue distribution of

chimeric 81C6 labeled with ^{211}At was determined in athymic mice with subcutaneous D-54 MG human glioma xenografts along with that of the radioiodinated mAb [192]. The uptake of ^{211}At in tumor increased with time and peaked at 16 h (20 ± 4% ID/g) and remained constant through 48 h. The accumulation of ^{211}At was similar to that of ^{131}I in most tissues except in spleen and stomach at some time points. However, the ^{211}At/^{131}I ratios were lower than that seen with mAb fragments suggesting that ^{211}At-ch81C6 is reasonably stable *in vivo*. The radiotoxicity of ^{211}At-ch81C6 was determined and its LD_{10} established from studies using the $B6C3F_1$ mouse strain [193]. The LD_{10} was found to be 45.7 kBq/g body weight in females and 101.5 kBq/g in males, equivalent to patient doses of 2.7 GBq and 7.1 GBq in females, and males, respectively. Toxic effects consisted of perivascular fibrosis of the intraventricular septum of the heart, bone marrow suppression, spermatic maturational delay, and splenic white pulp atrophy, and were seen in only a few animals receiving the highest doses of ^{211}At-ch81C6. The toxicity of intravenous ^{211}At-ch81C6 was about half observed for [^{211}At]astatide, which was speculated as reflecting differences in the homogeneity of dose deposition within critical organs.

81C6: Clinical Studies

A phase I study has been conducted with ^{211}At-ch81C6 in patients with recurrent malignant glioma to determine the feasibility, safety, and efficacy of this regimen [139,194]. Due to the lack of information regarding the behavior of α-particle-emitting endoradiotherapeutics, the study was conducted in a setting that would subject normal tissues to minimal exposure to ^{211}At—the agent was administered directly into a surgically created resection cavity (SCRC). In addition, direct administration into the SCRC rather than the intravenous injection should increase tumor dose and perhaps minimize catabolism of the labeled mAb in systemic organs.

A total of 18 patients (14 glioblastoma multiforme (GBM) (78%), 3 anaplastic oligodendroglioma (AO) (17%), and 1 anaplastic astrocytoma (AA) (5%)) were treated with escalating radioactivity levels of ^{211}At-ch81C6 (71-347 MBq) but with a constant amount (10 mg) of the mAb. As part of standard of care, these patients subsequently received salvage chemotherapy. Serial γ-camera imaging and blood sampling over 24 h after administration were performed to obtain pharmacokinetic data. A total of 96.7 ± 3.6% of the ^{211}At decays occurred within the cavity and the mean percent injected dose in the blood pool was ≤0.3 suggesting that leakage of radioactivity from the SCRC was minimal and that ^{211}At-ch81C6 was remarkably stable *in vivo*. None of the patients experienced dose-limiting toxicity. Within 6 weeks of ^{211}At-ch81C6 administration, six patients experienced grade 2 neurotoxicity that was resolved fully in all but 1 patient. The median survival times for all patients, those with GBM, and those with AA or AO were 54, 52, and 116 wk, respectively. These results demonstrate the feasibility of regionally targeted radiotherapy with ^{211}At-labeled agents and suggest that further evaluation of ^{211}At-ch81C6 in patients with CNS tumors is warranted.

DOSIMETRY AND MODELING

Absorbed dose calculations by conventional dosimetry assume a uniform radioactivity distribution within the tissues. However, due to the short range of α-particles, the absorbed dose and the corresponding therapeutic efficacy of an α-particle radiotherapeutic can be quite different if the radioactivity is not distributed uniformly, which is the norm than exception. Several microdosimetric models have been developed and applied to determine the absorbed dose of ^{211}At-labeled radiopharmaceuticals. It is beyond the scope of this review to cover all of these; instead, a few examples will be presented.

Vascular Targeting

A microdosimetric approach, based on two-dimensional histological images, was used to evaluate the therapeutic effectiveness of α-particle emitting ^{211}At and ^{213}Bi conjugated to 201B mAb, which targets lung vascular endothelial cells, in the treatment of EMT-6 lung tumor colonies in nude mice [195]. Autoradiography images were used to define the tissue morphology and the activity distribution within lung tissues. Probability density functions (*pdf*) were used to describe the variability in the average absorbed dose, $\hat{z}$, and normalized survival probability, $\hat{T}$, among tumor and normal cells. The *pdf* for the normalized survival probability, *pdf* ($\hat{T}$), was used to assess the overall survival fraction, *SF*, of tumor and normal tissue as a function of average cumulated activity concentration, $\tilde{q}$, in the tissue of interest. When the normalized average absorbed dose for a uniform activity distribution $\langle\hat{z}\rangle_u$ is set as a threshold, the *pdf* ($\hat{z}$) (*pdf* for $\hat{z}$) can be divided into the following regions: the under-dose fraction $F_<$ is the area where $\hat{z} < \langle\hat{z}\rangle_u$, and the over-dose fraction $F_>$ is the area where $\hat{z} > \langle\hat{z}\rangle_u$, and the zero-dose fraction F_0 is given when $\hat{z} = 0$. Two animal groups were studied, Group A with small tumors (< 130 μm), and Group B with larger tumors (< 600 μm). The average absorbed dose to tumor cells per unit cumulated activity concentration for animals in Group A was 1.10×10^{-3} and 1.37×10^{-3} Gy g MBq^{-1} s^{-1} for ^{211}At and ^{213}Bi, respectively, and for animals in Group B was 3.8×10^{-4} and 5.6×10^{-4} Gy g MBq^{-1} s^{-1} for ^{211}At and ^{213}Bi, respectively. The fraction of tumor cells that received a zero absorbed dose for animals in Group A was 0.04% for ^{213}Bi and 0.2% for ^{211}At, and for animals in Group B was 25% for ^{213}Bi and 31% for ^{211}At. Both ^{213}Bi and ^{211}At-labeled 201B mAb were effective therapies for animals with small tumors consistent with the prediction of the microdosimetric method; however, they were ineffective for animals with larger tumors. In summary, the microdosimetric methods based on knowledge of tissue morphology and activity distribution on a small-scale level can be a useful tool for evaluating *a priori* the therapeutic efficacy and limitations of targeted endoradiotherapeutic strategies.

HER2 Receptor

The EGF receptor HER2 is over expressed by 20-30% of human ovarian and breast carcinomas and is a valuable target for radionuclide therapy. The use of α-particle emitters might be an effective strategy because of the potential of these tumors to metastasize and spread as thin sheets in body compartments. However, little is known about the effects of heterogeneous target molecule expression on the potential effectiveness of α-particle-emitting radiotherapeutics. To evaluate this, the anti-HER2 mAb, trastuzumab was labeled with ^{211}At and its *in vitro* cytotoxicity was evaluated on 3 HER2 expressing breast cancer cell lines—SKBr-3, BT-474, and MCF-7/HER2 [167]. Analysis was carried out using a pharmacokinetic (PK) model that calculated the bound and internalized activity distribution among cell populations, based upon a) the competition of receptor sites between labeled and unlabeled monoclonal antibody and b) the heterogeneity of HER2 receptor expression, measured by FACS, among each cell line. The kinetics of ^{125}I-labeled Herceptin binding and internalization, and the average number of receptors per cell was determined, and the average cell and nuclear diameters were measured using an inverted microscope. Microdosimetry estimates were carried out using α-particle Monte Carlo transport with the nucleus considered to be the critical target. The estimated cell sensitivity z_0^{est} from the PK model based microdosimetry calculations was 0.29 Gy for SKBr-3, 0.355 Gy for MCF-7/HER2, and 0.63 Gy for BT-474 cells. In comparison, the D_{37} values measured for external beam radiation of these cells were 2.5, 3.1, and 6.1 Gy, respectively, indicating that the cytotoxicity of ^{211}At-labeled trastuzumab was about 10 times more effective than low-LET radiation. Although the receptor density, determined by Scatchard analyses, was similar for MCF-7/HER2 cells (1.41×10^6 receptors/cell) and BT-474 cells (1.72×10^6 receptors/cell), the distribution in receptor concentration varied considerably between the two cell lines, with a more homogeneous distribution observed for the BT-474 cell line. The shapes of the clonogenic survival curves for the two cell lines

were shown to be different consistent with the variations observed in HER2 receptor heterogeneity. The efficiency of cell killing for a higher specific activity ^{211}At-labeled trastuzumab preparation (45 kBq/μg) was better than for a low specific activity preparation (4.4 kBq/μg). Taken together, these studies indicate that specific activity and homogeneity of receptor expression are important parameters that affect cell killing.

Tumor-Associated Antigen on Colon Cancer Cells

Microdosimetric analysis of experimental data obtained from a study of the radiosensitivity of Colo-205 human colorectal cancer cells to irradiation from [^{211}At]astatide, [^{211}At]-albumin and [^{211}At]-C215 mAb in a slowly rotating, widely dispersed single cell suspension has been performed [196]. The aim of this study was to calculate the single cell specific energy values for the 3 labeled compounds and to determine the role of diffusion of ^{211}Po, the daughter nuclide created on the cell surface. The frequency-mean specific energy per event, $\bar{z}F$, was slightly higher when diffusion of the ^{211}Po atoms was included. The $\bar{z}F$ increased from 0.124 to 0.135 Gy for free ^{211}At irradiation and from 0.121 Gy to 0.132 Gy for ^{211}At-C215 irradiation when ^{211}Po diffusion was accounted for. For the ^{211}At-albumin irradiation, for which ^{211}Po diffusion is irrelevant, $\bar{z}F$ was 0.168 Gy. The mean specific energy and the single-cell radiosensitivity (z_{37}) for ^{211}At-albumin irradiation were 0.34 ± 0.06 Gy and 0.22 ± 0.07 Gy, respectively. For free ^{211}At irradiation, the value of z_{37} was 0.79 ± 0.17 Gy when the calculation was based on simulations where the ^{211}Po atoms created on the cell surface remained cell-bound. When these daughters were instead simulated to diffuse away from the cell, the calculated value of z_{37} was 0.44 ± 0.10 Gy. The corresponding values of z_{37} for ^{211}At-C215 irradiation were calculated to be 0.78 ± 0.08 Gy and 0.41 ± 0.05 Gy. These results show that ^{211}Po atoms will diffuse from the cell during its life-span. The increasing distance to the cell nucleus will drastically decrease the probability of the emitted alpha particle to hit the nucleus. This will result in fewer α-particle events in the cell nucleus. For dispersed cells, the diffusion of ^{211}Po atoms will reduce the total dose from cell-bound ^{211}At by a factor of 2.

PROBLEMS ASSOCIATED WITH ^{211}AT-LABELED RADIOTHERAPEUTICS

Supply of ^{211}At

Due to the scarcity of cyclotrons equipped with 25–30 MeV α-particle beams, which is a must for the production of ^{211}At, lack of radionuclide availability is a major impediment to the development of ^{211}At-labeled radiopharmaceuticals. Although considerable improvements have been made, the amount of astatine that can be produced may not be sufficient to meet routine clinical needs. Transportation of ^{211}At in the elemental form is a yet another issue; its relatively short half-life, volatility [197], loss of chemical reactivity with aging, and safety aspects are not conducive for its shipping. However, efforts are underway to facilitate the use of ^{211}At-radiotherapeutics at medical centers that do not posses a facility appropriate for ^{211}At production.

Radiolysis

Because ^{211}At is a relatively short-lived radionuclide that deposits large amounts of energy in a highly focal manner, it can inflict deleterious effects on the labeling chemistry and on the biological characteristics of the final labeled radiopharmaceuticals. Most of the astatinated radiopharmaceuticals reported are synthesized at a level of approximately 37 MBq. However, problems were encountered when the synthesis of SAB was attempted at a level that was necessary to produce about 370 MBq of the labeled mAb for the clinical study [198]. The radiochemical yields of SAB were reduced by about 2-fold and the immunoreactivity of the labeled mAb was unacceptable; in addition, the adhesion of the radioactivity to the reaction vessel was a problem. It should be pointed out that radiation dose-dependent loss of immunoreactivity of another ^{211}At-labeled mAb [199] and the fragmentation of ^{211}At-

polylysine [108] has been reported. Because the radiation dose delivered during the labeling procedure was in excess of 1,000 Gy, it was hypothesized that the α-particle irradiation must have decomposed the tin precursor and/or the SAB. An initial study was conducted investigating the stability of MeSTB and BuSTB, two tin precursors from which SAB can be derived, as a function of radiation dose in 3 different solvents [198]. The main conclusions drawn from this study are that chloroform, the solvent used for the clinical level synthesis of SAB, is very labile radiolytically and that the tin precursors underwent extensive decomposition as a function of the radiation dose with concomitant generation of an unidentified byproduct (Fig. **12**). It was speculated that this byproduct is *N*-succinimidyl 3-chlorobenzoate, presumably formed by the reaction of tin precursors with chlorine radicals generated from the radiolysis of chloroform. On the other hand, the tin precursors were stable to radiolysis in methanol and benzene. Further investigations of the effect of radiolysis on SAB synthesis revealed that degradation of the tin precursor is not the sole cause of reduced radiochemical yields [200]. It was speculated that, in methanol, production of reducing species by its radiolysis-induced disproportionation might be affecting the yields adversely either by consuming the oxidizing agent or converting the reactive astatine species to an inactive form. Although benzene is more radiolytically inert, it was found to be not a good solvent for astatination chemistry. This is due to the formation of, most likely, astatobenzene by the reaction of reactive astatine with benzene presumably at a faster rate than with the tin precursor. A suggested alternative for the production of higher amounts of astatinated radiopharmaceuticals is the split and pool approach. From yet another study, it was shown that, with increasing radiation dose, the reactive form of astatine is gradually converted to an inactive form, presumably astatide; however, it could not be converted back to the reactive form in sufficient amounts by treatment with the oxidizing agent NCS [201]. Taken together, the results of these studies underscore the potential importance of radiolysis-mediated effects on the chemistry of α-particle–emitting radiopharmaceuticals and the need to evaluate labeling chemistry at the high radiation doses required for clinical use.

In Vivo Stability

Compared to their radioiodinated counterparts, astatinated radiopharmaceuticals are generally more unstable *in vivo* presumably due to weaker carbon-astatine bond strength. Combined with their extreme cytotoxicity, this makes them less suitable for systemic administrations. Thyroid, spleen, lungs and stomach sequester free astatide preferentially and efforts have been taken to block uptake of astatide by these tissues [202]. Of the seven agents studied, monovalent ions iodide, thiocyanate and perchlorate reduced uptake in thyroid and stomach. On the other hand, with the exception of thiocyanate, these agents did not have significant effect on the uptake of astatide in lungs and spleen. The sulfhydryl-containing compounds were less effective in reducing the uptake of astatide by various normal tissues. Thiocyanate also helped to reduce the astatide accumulation in blood and kidneys suggesting it was the best compound for reducing the uptake of astatide in normal tissues. Lysine has been shown to have an additive effect in the reduction by thiocyanate of astatide uptake in stomach [122]. These studies show that while such blocking strategies may augment the clinical utility of ^{211}At-labeled therapeutics, multiple agents may be necessary.

CONCLUSION AND FUTURE PROSPECTS

Notwithstanding the limitations of astatine-211, considerable progresses has been made to exploit its useful features for targeted alpha particle therapy including a successful clinical trial of ^{211}At-labeled mAb. Areas that still need further development include the routine production of astatine-211 at a scale useful for clinical applications, means to overcome the harmful effects of radiolysis on radiosynthesis at higher doses, and chemistries with which molecules can be labeled with ^{211}At in a stable form so that the final therapeutic can be administered

systemically. We strongly feel that efforts that are under way at various institutions around the world will yield fruitful strategies for overcoming these problems and permit the promise of astatinated radiotherapeutics for cancer treatment to be more fully realized.

Acknowledgments

Funding for the work performed in the authors' laboratories was provided by Grants CA42324 and NS20023 from National Institutes of Health.

REFERENCES

1. Davies AJ. Oncogene 2007;26:3614. [PubMed: 17530015]
2. Macklis RM. Semin. Radiat. Oncol 2007;17:176. [PubMed: 17591564]
3. Humm JL. J. Nucl. Med 1986;27:1490. [PubMed: 3528417]
4. Sautter-Bihl M-L, Herbold G, Bihl H. Recent Results Cancer Res 1996;141:67. [PubMed: 8722420]
5. Hall, E.; Giaccia, AJ. Radiobiology for the Radiologist. 6th edition. Lippincott Williams & Wilkins; Philadelphia: 2006.
6. Kampf G. Radiobiol. Radiother. (Berl) 1988;29:631–58. [PubMed: 3253788]
7. Rotmensch J, Whitlock JL, Schwartz JL, Hines JJ, Reba RC, Harper PV. Am. J. Obstet. Gynecol 1997;176:833. [PubMed: 9125608]
8. Song YJ, Qu CF, Rizvi SM, Li Y, Robertson G, Raja C, Morgenstern A, Apostolidis C, Perkins AC, Allen BJ. Cancer Lett 2006;234:176. [PubMed: 15961220]
9. Nilsson S, Larsen RH, Fossa SD, Balteskard L, Borch KW, Westlin JE, Salberg G, Bruland OS. Clin. Cancer Res 2005;11:4451. [PubMed: 15958630]
10. Antczak C, Jaggi JS, LeFave CV, Curcio MJ, McDevitt MR, Scheinberg DA. Bioconjugate Chem 2006;17:1551.
11. Jaggi JS, Henke E, Seshan SV, Kappel BJ, Chattopadhyay D, May C, McDevitt MR, Nolan D, Mittal V, Benezra R, Scheinberg DA. PLoS ONE 2007;2:e267. [PubMed: 17342201]
12. Zalutsky MR, Vaidyanathan G. Curr. Pharm. Des 2000;6:1433. [PubMed: 10903402]
13. Vaidyanathan G, Zalutsky MR. Phys. Med. Biol 1996;41:1915. [PubMed: 8912371]
14. Weinreich, R. Molecular Therapy with ^{211}At. In: Amaldi, U.; Larrson, B.; Lemoigne, Y., editors. Advances in Hadrontherapy. Elsevier; New York: 1997. p. 359-382.
15. Corson DR, MacKenzie KR, Segre E. Phys. Rev 1940;58:672.
16. Johnson EL, Turkington TG, Jaszczak RJ, Gilland DR, Vaidyanathan G, Greer KL, Coleman RE, Zalutsky MR. Nucl. Med. Biol 1995;22:45. [PubMed: 7735169]
17. Turkington TG, Zalutsky MR, Jaszczak RJ, Garg PK, Vaidyanathan G, Coleman RE. Phys. Med. Biol 1993;38:1121. [PubMed: 8367523]
18. Tolmachev V, Carlsson J, Lundqvist H. Acta Oncol 2004;43:264. [PubMed: 15244250]
19. Larsen RH, Wieland BW, Zalutsky MR. Appl. Radiat. Isot 1996;47:135. [PubMed: 8852627]
20. Lebeda O, Jiran R, Ralis J, Stursa J. Appl. Radiat. Isot 2005;63:49. [PubMed: 15866447]
21. Lindegren S, Back T, Jensen HJ. Appl. Radiat. Isot 2001;55:157. [PubMed: 11393754]
22. Henriksen G, Messelt S, Olsen E, Larsen RH. Appl. Radiat. Isot 2001;54:839. [PubMed: 11258534]
23. Groppi F, Bonardi ML, Birattari C, Menapace E, Abbas K, Holzwarth U, Alfarano A, Morzenti S, Zona C, Alfassi ZB. Appl. Radiat. Isot 2005;63:621. [PubMed: 16055338]
24. Alfarano A, Abbas K, Holzwarth U, Bonardi M, Groppi F, Alfassi Z, Menapace E, Gibson PN. J. Phys. Conferences series 2006;41:115.
25. Casarett GW. Radiat. Res 1964;51(SUPPL 5):246. [PubMed: 14217563]
26. Schultz MK, Hammond M, Cessna JT, Plascjak P, Norman B, Szajek L, Garmestani K, Zimmerman BE, Unterweger M. Appl. Radiat. Isot 2006;64:1365. [PubMed: 16563782]
27. Hermanne A, Tarkanyi F, Takacs S, Szucs Z, Shubin YN, Dityuk AI. Appl. Radiat. Isot 2005;63:1. [PubMed: 15866442]
28. Zalutsky MR, Zhao XG, Alston KL, Bigner D. J. Nucl. Med 2001;42:1508. [PubMed: 11585865]

29. Yordanov AT, Pozzi O, Carlin S, Akabani G, Wieland B, Zalutsky MR. J. Radioanal. Nucl. Chem 2004;262:593.
30. Roy K, Basu S, Ramaswami A, Nayak D, Lahiri S. Appl. Radiat. Isot 2004;60:793. [PubMed: 15110342]
31. Berei, K.; Eberle, SH.; Kirby, HW.; Münzel, H.; Rössler, K.; Seidel, A.; Vasáros, L. Gmelin Handbook of Inorganic Chemistry - Astatine. Springer-Verlag; Berlin: 1985.
32. Brown I. Adv. Inrog. Chem 1987;31:43.
33. Ludwig R, Dreyer R, Fischer S. Radiochim. Acta 1989;47:129.
34. Visser GWM. Radiochim. Acta 1989;47:97.
35. Coenen HH, Moerlein SM, Stocklin G. Radiochim. Acta 1983;34:47.
36. Vedeneyev, VI.; Gurvich, LV.; Kondrat'yev, VN.; Medvedev, VA.; Frankevich, YL. Bond Energies, Ionization Potentials, and Electron Affinities. St. Martin's Press; New York: 1966.
37. McLendon RE, Archer GE, Larsen RH, Akabani G, Bigner DD, Zalutsky MR. Int. J. Radiat. Oncol. Biol. Phys 1999;45:491. [PubMed: 10487576]
38. Bloomer WD, McLaughlin WH. Radiochim. Acta 1989;47:149.
39. Pillai KMR, Mclaughlin WH, Lambrecht RM, Bloomer WD. J. Label. Compd. Radiopharm 1987;24:1117.
40. Sven D. ZfI-Mitteilungen 1991;165:96.
41. Brown I. Radiochem. Radioanal. Lett 1982;53:343.
42. Shiue CY, Meyer GJ, Ruth TJ, Wolf AP. J. Label. Compd. Radiopharm 1981;18:1039.
43. Vasaros L, Norsevev YV, Nhan DD, Khalkin VA. Radiochem. Radioanal. Lett 1982;50:275.
44. Vasaros L, Norseyev YV, Nhan DD, Khalkin VA. Radiochem. Radioanal. Lett 1981;47:403.
45. Vasaros L, Norseyev YV, Nhan DD, Khalkin VA. Radiochem. Radioanal. Lett 1981;47:313.
46. Vasaros L, Norseev IV, Khalkin VA. Doklady Akademii Nauk Sssr 1982;266:120.
47. Norseev YV, Dang DN, Khalkin VA, Huan NQ, Vasaros L. J.Radioanal. Nucl. Chem 1985;94:185.
48. Visser GWM, Diemer EL, Kaspersen FM. Int. J. Appl. Radiat. Isot 1979;30:749.
49. Sriyapureddy SS, Meyer GJ, Krull D, Matzke KH, Knapp WH. J. Label. Compd. Radiopharm 2007;50:S279.
50. Zalutsky, MR. Antibody-mediated Radiotherapy: Future Prospects. In: Zalutsky, MR., editor. Antibodies in Radiodiagnosis and Therapy. CRC Press; Boca Raton: 1989. p. 213-235.
51. Kaderavek J, Leseticky L, Kozempel J, Lebeda O. J. Label. Compd. Radiopharm 2007;50:S272.
52. Visser GWM, Diemer EL, Kaspersen FM. J. Label. Compd. Radiopharm 1981;18:799.
53. Vaidyanathan G, Zalutsky MR. Bioconjugate Chem 1992;3:499.
54. Vaidyanathan G, Affleck DJ, Alston KL, Zalutsky MR. J. Label. Compd. Radiopharm 2007;50:177.
55. Vaidyanathan G, Affleck DJ, Schottelius M, Wester H, Friedman HS, Zalutsky MR. Bioconjugate Chem 2006;17:195.
56. Talanov VS, Garmestani K, Regino CA, Milenic DE, Plascjak PS, Waldmann TA, Brechbiel MW. Nucl. Med. Biol 2006;33:469. [PubMed: 16720238]
57. Visser GWM, Diemer EL, Kaspersen FM. Int. J. Appl. Radiat. Isot 1982;33:389.
58. Milius RA, McLaughlin WH, Lambrecht RM, Wolf AP, Carroll JJ, Adelstein SJ, Bloomer WD. Int. J. Appl. Radiat. Isot 1986;37:799.
59. Wilbur DS, Chyan MK, Hamlin DK, Vessella RL, Wedge TJ, Hawthorne MF. Bioconjugate Chem 2007;18:1226.
60. Milesz S, Jovchev M, Schumann D, Khalkin VA, Milanov M. J. Radioanal. Nucl. Chem. Lett 1988;127:193.
61. Yordanov AT, Deal K, Garmestani K, Kobayashi H, Herring B, Waldman TA, Brechbiel MW. J. Label. Compd. Radiopharm 2000;43:1219.
62. Liu N, Jin JN, Mo SW, Chen HL, Yu YP. J.Radioanal. Nucl. Chem 1998;227:187.
63. Liu NJ, Mo S, Chen H, Yu Y. He Huaxue Yu Fangshe Huaxue 1998;20:158.
64. Norseyev YVS. Nukleonika 1995;40:13.
65. Pruszynski M, Bilewicz A, Zalutsky MR. J. Label. Compd. Radiopharm 2007;50:S32.

66. Pruszynski M, Bilewicz A, Zalutsky MR. Eur. J. Nucl. Med. Mol. Imaging 2007;34:210.
67. Pruszynski M, Bilewicz A, Was B, Petelenz B. J. Radioanal. Nucl. Chem 2006;268:91.
68. Garg PK, Harrison CL, Zalutsky MR. Cancer Res 1990;50:3514. [PubMed: 2340501]
69. Brown I, Carpenter RN. Acta Radiologica 1991;25:351.
70. Brown I, Carpenter RN. Clin. Radiol 1988;39:353.
71. Brown I, Carpenter RN. Eur. J.Nucl. Med 1988;14:234.
72. Lundh C, Lindencrona U, Schmitt A, Nilsson M, Forssell-Aronsson E. Cancer Biother. Radiopharm 2006;21:591. [PubMed: 17257074]
73. Carlin S, Akabani G, Zalutsky MR. J. Nucl. Med 2003;44:1827. [PubMed: 14602867]
74. Carlin S, Mairs RJ, Welsh P, Zalutsky MR. Nucl. Med. Biol 2002;29:729. [PubMed: 12381453]
75. Petrich T, Helmeke HJ, Meyer GJ, Knapp WH, Potter E. Eur. J. Nucl. Med.Mol. Imaging 2002;29:842. [PubMed: 12111124]
76. Petrich T, Quintanilla-Martinez L, Korkmaz Z, Samson E, Helmeke HJ, Meyer GJ, Knapp WH, Potter E. Clin. Cancer Res 2006;12:1342. [PubMed: 16489092]
77. Lindencrona U, Forssell-Aronsson E, Nilsson M. Nucl. Med. Biol 2007;34:523. [PubMed: 17591552]
78. Lindencrona U, Nilsson M, Forssell-Aronsson E. Nucl. Med. Biol 2001;28:41. [PubMed: 11182563]
79. Bloomer WD, McLaughlin WH, Lambrecht RM, Atcher RW, Mirzadeh S, Madara JL, Milius RA, Zalutsky MR, Adelstein SJ, Wolf AP. Int. J. Radiat. Oncol. Biol. Phys 1984;10:341. [PubMed: 6706730]
80. Bloomer WD, Mclaughlin WH, Neirinckx RD, Adelstein SJ, Gordon PR, Ruth TJ, Wolf AP. Science 1981;212:340. [PubMed: 7209534]
81. Larsen RH, Hoff P, Vergote IB, Bruland OS, Aas M, De Vos L, Nustad K. Gynecol. Oncol 1995;57:9. [PubMed: 7705707]
82. Larsen RH, Varaas T, Hoff P, Vergote IB, Alstad J, De-Vos LN, Nustad K. J. Label. Compd. Radiopharm 1996;38:775.
83. Bredow J, Kretzschmar M, Wunderlich G, Dorr W, Pohl T, Franke WG, Kotzerke J. Nuklearmedizin 2004;43:63. [PubMed: 15029267]
84. Doberenz I, Doberenz W, Wunderlich G, Franke W-G, Heidelbach JG, Fischer S, Dreyer R, Kessler L. NucCompact 1990;21:124.
85. Kucka J, Hruby M, Konak C, Kozempel J, Lebeda O. Appl. Radiat. Isot 2006;64:201. [PubMed: 16154358]
86. Hartman KB, Hamlin DK, Wilbur DS, Wilson LJ. Small 2007;3:1496. [PubMed: 17668431]
87. Mougin-Degraef M, Jestin E, Bruel D, Remaud-Le Saec P, Morandeau L, Faivre-Chauvet A, Barbet J. J. Liposome Res 2006;16:91. [PubMed: 16556552]
88. Shmakova NLK, Norseev Yu. V. Fadeeva TA, Krasavin EA, Kodina GE, Gol'tyapin Yu. V. Sorokin VP, Slobodyanik II, Korsunskii VN. Meditsinskaya Radiolo. Radiatsionnaya Bezopasnost 2002;47:5.
89. Norseev YV. J. Radioanal. Nucl. Chem 1998;237:155.
90. Roessler K, Meyer GJ, Stoecklin G. J. Label. Compd. Radiopharm 1977;13:271.
91. Vaidyanathan G, Larsen RH, Zalutsky MR. Cancer Res 1996;56:1204. [PubMed: 8640798]
92. Koziorowski J, Lebeda O, Weinreich R. Appl. Radiat. Isot 1999;50:527.
93. Koziorowski J, Weinreich R. J. Radioanal. Nucl. Chem 1997;219:127.
94. Larsen RH, Vaidyanathan G, Zalutsky MR. Int. J. Radiat. Biol 1997;72:79. [PubMed: 9246197]
95. Walicka MA, Vaidyanathan G, Zalutsky MR, Adelstein SJ, Kassis AI. Radiat. Res 1998;150:263. [PubMed: 9728654]
96. Vaidyanathan G, Zalutsky MR. Nucl. Med. Biol 1998;25:487. [PubMed: 9720667]
97. Vaidyanathan G, Affleck DJ, Alston KL, Zhao XG, Hens M, Hunter DH, Babich J, Zalutsky MR. Bioorg. Med. Chem 2007;15:3430. [PubMed: 17387017]
98. Vaidyanathan G, Strickland DK, Zalutsky MR. Int. J. Cancer 1994;57:908. [PubMed: 8206683]
99. Vaidyanathan G, Friedman HS, Keir ST, Zalutsky MR. Nucl Med Biol 1996;23:851–6. [PubMed: 8940730]

100. Strickland DK, Vaidyanathan G, Zalutsky MR. Cancer Res 1994;54:5414. [PubMed: 7923174]
101. Strickland DK, Vaidyanathan G, Friedman HS, Zalutsky MR. J. Neuro-Oncol 1995;25:9.
102. Cunningham SH, Mairs RJ, Wheldon TE, Welsh PC, Vaidyanathan G, Zalutsky MR. Br. J. Cancer 1998;77:2061. [PubMed: 9649115]
103. Boyd M, Mairs RJ, Keith WN, Ross SC, Welsh P, Akabani G, Owens J, Vaidyanathan G, Carruthers R, Dorrens J, Zalutsky MR. J. Gene Med 2004;6:937. [PubMed: 15293352]
104. Boyd M, Ross SC, Dorrens J, Fullerton NE, Tan KW, Zalutsky MR, Mairs RJ. J. Nucl. Med 2006;47:1007. [PubMed: 16741311]
105. O McCarthy H, Worthington J, Barrett E, Cosimo E, Boyd M, Mairs RJ, Ward C, McKeown SR, Hirst DG, Robson T. Gene Ther 2007;14:246. [PubMed: 17006546]
106. Vaidyanathan G, Affleck DJ, Zalutsky MR. Bioconjugate Chem 1996;7:102.
107. Vaidyanathan G, Zhao XG, Larsen RH, Zalutsky MR. Br. J. Cancer 1997;76:226. [PubMed: 9231923]
108. Lindegren S, Andersson H, Jacobsson L, Back T, Skarnemark G, Karlsson B. Bioconjugate Chem 2002;13:502.
109. Lindegren S, Karlsson B, Jacobsson L, Andersson H, Hultborn R, Skarnemark G. Clin. Cancer Res 2003;9:3873S. [PubMed: 14506185]
110. Wilbur DS, Hamlin DK, Chyan MK, Kegley BB, Quinn J, Vessella RL. Bioconjugate Chem 2004;15:601.
111. Murud KM, Larsen RH, Hoff P, Zalutsky MR. Nucl. Med. Biol 1999;26:397. [PubMed: 10382843]
112. Murud KM, Larsen RH, Bruland OS, Hoff P. Nuc. Med. Biol 1999;26:791.
113. Larsen RH, Murud KM, Akabani G, Hoff P, Bruland OS, Zalutsky MR. J. Nucl. Med 1999;40:1197. [PubMed: 10405142]
114. Garg PK, John CS, Zalutsky MR. Nucl. Med. Biol 1995;22:467. [PubMed: 7550023]
115. Brevik EM, Lrstad E, Hoff P. Czech. J. Phys 2003;53:A725.
116. Liu BL, Jin YT, Liu ZH, Luo C, Kojima M, Maeda M. Int. J. Appl. Radiat. Isot 1985;36:561. [PubMed: 2933343]
117. Vaidyanathan G, Affleck D, Welsh P, Srinavasan A, Schmidt M, Zalutsky MR. Nuc. Med. Biol 2000;27:329.
118. Vaidyanathan G, Boskovitz A, Shankar S, Zalutsky MR. Peptides 2004;25:2087. [PubMed: 15572196]
119. Liu N, Yang YY, Zan LB, Liao JL, Jin JN. J. Radioanal. Nucl. Chem 2007;272:85.
120. Nilsson FY, Tolmachev V. Curr. Opinion Drug Disc. Develop 2007;10:167.
121. Tolmachev V, Orlova A, Nilsson FY, Feldwisch J, Wennborg A, Abrahmsen L. Expert Opinion Biol. Ther 2007;7:555.
122. Steffen AC, Almqvist Y, Chyan MK, Lundqvist H, Tolmachev V, Wilbur DS, Carlsson J. Oncol. Reports 2007;17:1141.
123. Sjostrom A, Tolmachev V, Lebeda O, Koziorowski J, Carlsson J, Lundqvist H. J. Radioanal. Nuclear Chem 2003;256:191.
124. Sundberg AL, Almqvist Y, Tolmachev V, Carlsson J. Eur. J. Nucl. Med. Mol. Imaging 2003;30:727. [PubMed: 12740721]
125. Sundberg AL, Almqvist Y, Orlova A, Blomquist E, Jensen HJ, Gedda L, Tolmachev V, Carlsson J. Eur. .J Nucl. Med. Mol. Imaging 2003;30:1348. [PubMed: 12937952]
126. Sundberg AL, Steffen AC. Int. J. Radiat. Oncol. Biol. Phys 2007;67:279. [PubMed: 17189076]
127. Orlova A, Sjostrom A, Lebeda O, Lundqvist H, Carlsson J, Tolmachev V. Anticancer Res 2004;24:4035. [PubMed: 15736449]
128. Aaij C, Tschroots WR, Lindner L, Feltkamp TE. Int. J. Appl. Radiat. Isot 1975;26:25. [PubMed: 1110103]
129. Visser GWM, Diemer EL, Kaspersen FM. Int. J. Appl. Radiat. Isot 1980;31:275.
130. Friedman AM, Zalutsky MR, Wung W, Buckingham F, Harper PV, Scherr GH, Wainer B, Hunter RL, Appelman EH, Rothberg RM, Fitch FW, Stuart FP, Simonian SJ. Int. J. Nucl. Med. Biol 1977;4:219. [PubMed: 608810]

131. Vaughan ATM. Int. J. Appl. Radiat. Isot 1979;30:576.
132. Harrison A, Royle L. Int. J. Appl.Radiat. Isot 1984;35:1005. [PubMed: 6526518]
133. Yi CH, Jin J, Zhang SY, Wang KT, Zhang DY, Zhou ML. J. Radioanal. Nucl. Chem 1989;129:377.
134. Liu N, Jin J, Zhang S, Mo S, Yang Y, Wang J, Zhou M. J. Radioanal. Nucl. Chem 2001;247:129.
135. Liu N, Jin JN, Zhang SY, Luo DY, Wang JA, Zou ML, Luo L, Wang FY. J. Label. Compd. Radiopharm 1995;36:1105.
136. Zalutsky MR, Narula AS. Appl. Radiat. Isot 1988;39:227.
137. Wilbur DS, Hylarides MD, Fritzberg AR. Radiochim. Acta 1989;47:137.
138. Boskovitz A, Akabani G, Zhao XG, Alston K, Zalutsky MR. Clin. Cancer Res 2003;9:6189S.
139. Zalutsky MR, Reardon DA, Pozzi OR, Vaidyanathan G, Bigner DD. Nucl. Med. Biol 2007;34:779. [PubMed: 17921029]
140. Steffen AC, Almqvist Y, Chyan MK, Lundqvist H, Tolmachev V, Wilbur DS, Carlsson J. Oncol. Rep 2007;17:1141. [PubMed: 17390057]
141. Wilbur DS, Chyan MK, Hamlin DK, Kegley BB, Risler R, Pathare PM, Quinn J, Vessella RL, Foulon C, Zalutsky M, Wedge TJ, Hawthorne MF. Bioconjugate Chem 2004;15:203.
142. Zalutsky MR, Garg PK, Friedman HS, Bigner DD. Proc. Natl. Acad. Sci. USA 1989;86:7149. [PubMed: 2476813]
143. Cheng JP, Ekberg T, Engstrom M, Nestor M, Jensen HJ, Tolmachev V, Anniko M. Laryngoscope 2007;117:1013. [PubMed: 17440426]
144. Walte A, Sriyapureddy SS, Korkmaz Z, Krull D, Bolte O, Hofmann M, Meyer GJ, Knapp WH. J. Pharm. Pharmaceut. Sci 2007;10:277s.
145. Demartis S, Tarli L, Borsi L, Zardi L, Neri D. Eur. J. Nucl. Med 2001;28:534. [PubMed: 11357506]
146. Vaidyanathan G, Affleck D, Zalutsky MR. Nucl. Med. Biol 1994;21:105. [PubMed: 9234271]
147. Talanov VS, Yordanov AT, Garmestani K, Milenic DE, Arora HC, Plascjak PS, Eckelman WC, Waldmann TA, Brechbiel MW. Nucl. Med. Biol 2004;31:1061. [PubMed: 15607488]
148. Yordanov AT, Garmestani K, Zhang M, Zhang Z, Yao Z, Phillips KE, Herring B, Horak E, Beitzel MP, Schwarz UP, Gansow OA, Plascjak PS, Eckelman WC, Waldmann TA, Brechbiel MW. Nucl. Med. Biol 2001;28:845. [PubMed: 11578907]
149. Reist CJ, Foulon CF, Alston K, Bigner DD, Zalutsky MR. Nucl. Med. Biol 1999;26:405. [PubMed: 10382844]
150. Vaidyanathan G, Affleck DJ, Bigner DD, Zalutsky MR. Nucl. Med. Biol 2003;30:351. [PubMed: 12767391]
151. Wilbur DS, Hamlin DK, Chyan MK, Brechbiel MW. Bioconjugate Chem 2008;19:158.
152. Milesz S, Norseev YV, Szucs Z, Vasaros L. J. Radioanal. Nucl. Chem. Lett 1989;137:365.
153. Vaughan AT, Bateman WJ, Brown G, Cowan J. Int. J. Nucl. Med. Biol 1982;9:167. [PubMed: 6957405]
154. Larsen RH, Bruland OS, Hoff P, Alstad J, Lindmo T, Rofstad EK. Radiat. Res 1994;139:178. [PubMed: 8052693]
155. Larsen RH, Bruland OS, Hoff P, Alstad J, Rofstad EK. Br. J. Cancer 1994;69:1000. [PubMed: 8198960]
156. Aurlien E, Kvinnsland Y, Larsen RH, Bruland OS. Int. J. Radiat. Biol 2002;78:133. [PubMed: 11779363]
157. Larsen RH, Akabani G, Welsh P, Zalutsky MR. Radiat. Res 1998;149:155. [PubMed: 9457895]
158. Hauck ML, Larsen RH, Welsh PC, Zalutsky MR. Br. J. Cancer 1998;77:753. [PubMed: 9514054]
159. Aurlien E, Larsen RH, Kvalheim G, Bruland OS. Br. J. Cancer 2000;83:1375. [PubMed: 11044364]
160. Andersson H, Elgqvist J, Horvath G, Hultborn R, Jacobsson L, Jensen H, Karlsson B, Lindegren S, Palm S. Clin. Cancer Res 2003;9:3914S. [PubMed: 14506189]
161. Andersson H, Lindegren S, Back T, Jacobsson L, Leser G, Horvath G. Acta Oncol 2000;39:741. [PubMed: 11130014]
162. Andersson H, Lindegren S, Back T, Jacobsson L, Leser G, Horvath G. Anticancer Res 2000;20:459. [PubMed: 10769696]

163. Andersson H, Palm S, Lindegren S, Back T, Jacobsson L, Leser G, Horvath G. Anticancer Res 2001;21:409. [PubMed: 11299770]
164. Elgqvist J, Andersson H, Back T, Hultborn R, Jensen H, Karlsson B, Lindegren S, Palm S, Warnhammar E, Jacobsson L. J. Nucl. Med 2005;46:1907. [PubMed: 16269606]
165. Nestor M, Persson M, van Dongen GA, Jensen HJ, Lundqvist H, Anniko M, Tolmachev V. Eur. J. Nucl. Med. Mol. Imaging 2005;32:1296. [PubMed: 16028065]
166. Palm S, Back T, Claesson I, Delle U, Hultborn R, Lindegren S, Jacobsson L. Anticancer Res 2003;23:1219. [PubMed: 12820374]
167. Akabani G, Carlin S, Welsh P, Zalutsky MR. Nucl. Med. Biol 2006;33:333. [PubMed: 16631082]
168. Bateman WJ, Vaughan AT, Brown G. Int. J. Nucl. Med. Biol 1983;10:241. [PubMed: 6582053]
169. Vaughan AT, Bateman WJ, Fisher DR. Int. J. Radiat. Oncol. Biol. Phys 1982;8:1943. [PubMed: 6295988]
170. Harrison A, Royle L. NCI Monogr 1987:157. [PubMed: 3493441]
171. Zalutsky MR, Garg PK, Friedman HS, Bigner DD. Proc. Natl. Acad. Sci. USA 1989;86:7149. [PubMed: 2476813]
172. Garg, PK.; Bigner, DD.; Zalutsky, MR. Monoclonal Antibodies—Applications in Clinical Oncology. Epenetos, AA., editor. Chapman and Hall; London: 1991. p. 103-114.
173. Cope DA, Dewhirst MW, Friedman HS, Bigner DD, Zalutsky MR. Cancer Res 1990;50:1803. [PubMed: 2407344]
174. Hadley SW, Wilbur DS, Gray MA, Atcher RW. Bioconjugate Chem 1991;2:171.
175. Wilbur DS, Vessella RL, Stray JE, Goffe DK, Blouke KA, Atcher RW. Nucl. Med. Biol 1993;20:917. [PubMed: 8298571]
176. Andersson H, Lindegren S, Back T, Jacobsson L, Leser G, Horvath G. Anticancer Res 2000;20:459. [PubMed: 10769696]
177. Andersson H, Lindegren S, Back T, Jacobsson L, Leser G, Horvath G. Acta Oncol 2000;39:741. [PubMed: 11130014]
178. Andersson H, Palm S, Lindegren S, Back T, Jacobsson L, Leser G, Horvath G. Anticancer Res 2001;21:409. [PubMed: 11299770]
179. Elgqvist J, Bernhardt P, Hultborn R, Jensen H, Karlsson B, Lindegren S, Warnhammar E, Jacobsson L. J. Nucl. Med 2005;46:464. [PubMed: 15750160]
180. Back T, Andersson H, Divgi CR, Hultborn R, Jensen H, Lindegren S, Palm S, Jacobsson L. J. Nucl. Med 2005;46:2061. [PubMed: 16330571]
181. Elgqvist J, Andersson H, Back T, Claesson I, Hultborn R, Jensen H, Johansson BR, Lindegren S, Olsson M, Palm S, Warnhammar E, Jacobsson L. J. Nucl. Med 2006;47:1342. [PubMed: 16883015]
182. Elgqvist J, Andersson H, Bernhardt P, Back T, Claesson I, Hultborn R, Jensen H, Johansson BR, Lindegren S, Olsson M, Palm S, Warnhammar E, Jacobsson L. Int. J. Radiat. Oncol. Biol. Phys 2006;66:1228. [PubMed: 17145538]
183. Elgqvist J, Andersson H, Back T, Claesson I, Hultborn R, Jensen H, Lindegren S, Olsson M, Palm S, Warnhammar E, Jacobsson L. Nucl. Med. Biol 2006;33:1065. [PubMed: 17127181]
184. Palm S, Back T, Claesson I, Danielsson A, Elgqvist J, Frost S, Hultborn R, Jensen H, Lindegren S, Jacobsson L. Int. J. Radiat. Oncol. Biol. Phys 2007;69:572. [PubMed: 17869670]
185. Zhang Z, Zhang ML, Garmestani K, Talanov VS, Plascjak PS, Beck B, Goldman C, Brechbiel MW, Wadmann TA. Blood 2006;108:1007. [PubMed: 16569769]
186. Zhang M, Yao Z, Zhang Z, Garmestani K, Talanov VS, Plascjak PS, Yu S, Kim HS, Goldman CK, Paik CH, Brechbiel MW, Carrasquillo JA, Waldmann TA. Cancer Res 2006;66:8227. [PubMed: 16912202]
187. Zhang M, Yao Z, Patel H, Garmestani K, Zhang Z, Talanov VS, Plascjak PS, Goldman CK, Janik JE, Brechbiel MW, Waldmann TA. Proc. Natl. Acad. Sci. USA 2007;104:8444. [PubMed: 17488826]
188. Orlova A, Hoglund J, Lubberink M, Lebeda O, Gedda L, Lundqvist H, Tolmachev V, Sundin A. Cancer Biother. Radiopharm 2002;17:385. [PubMed: 12396703]
189. Kennel SJ, Mirzadeh S, Eckelman WC, Waldmann TA, Garmestani K, Yordanov AT, Stabin MG, Brechbiel MW. Radiat. Res 2002;157:633. [PubMed: 12005541]

190. Robinson MK, Shaller C, Garmestani K, Plascjak PS, Hodge KM, Yuan QA, Marks JD, Waldmann TA, Brechbiel MW, Adams GP. Clin. Cancer Res 2008;14:875. [PubMed: 18245551]

191. Zalutsky MR, McLendon RE, Garg PK, Archer GE, Schuster JM, Bigner DD. Cancer Res 1994;54:4719. [PubMed: 8062270]

192. Zalutsky MR, Stabin MG, Larsen RH, Bigner DD. Nucl. Med. Biol 1997;24:255. [PubMed: 9228660]

193. McLendon RE, Archer GE, Larsen RH, Akabani G, Bigner DD, Zalutsky MR. Int. J. Radiat. Oncol. Biol. Phys 1999;45:491. [PubMed: 10487576]

194. Zalutsky MR, Reardon DA, Akabani G, Coleman RE, Friedman AH, Friedman HS, McLendon RE, Wong TZ, Bigner DD. J. Nucl. Med 2008;49:30. [PubMed: 18077533]

195. Akabani G, Kennel SJ, Zalutsky MR. J. Nucl. Med 2003;44:792. [PubMed: 12732682]

196. Palm S, Humm JL, Rundqvist R, Jacobsson L. Med. Phys 2004;31:218. [PubMed: 15000607]

197. Lindencrona U, Sillfors-Elverby L, Nilsson M, Forssell-Aronsson E. Appl. Radiat. Isot 2005;62:395. [PubMed: 15607915]

198. Pozzi OR, Zalutsky MR. J. Nucl. Med 2005;46:700. [PubMed: 15809494]

199. Larsen RH, Bruland OS. J. Label. Compd. Radiopharm 1995;36:1009.

200. Pozzi OR, Zalutsky MR. J. Nucl. Med 2005;46:1393. [PubMed: 16085599]

201. Pozzi OR, Zalutsky MR. J. Nucl. Med 2007;48:1190. [PubMed: 17574991]

202. Larsen RH, Slade S, Zalutsky MR. Nucl. Med. Biol 1998;25:351. [PubMed: 9639296]

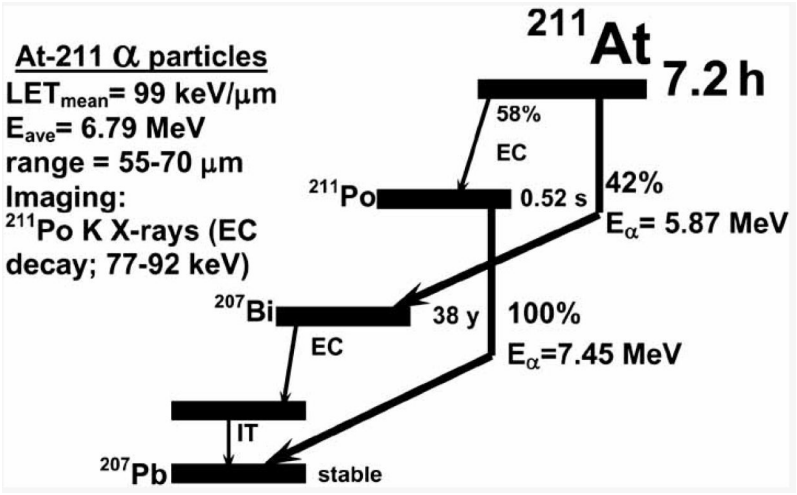

Fig (1).
Scheme for the nuclear decay of astatine-211.

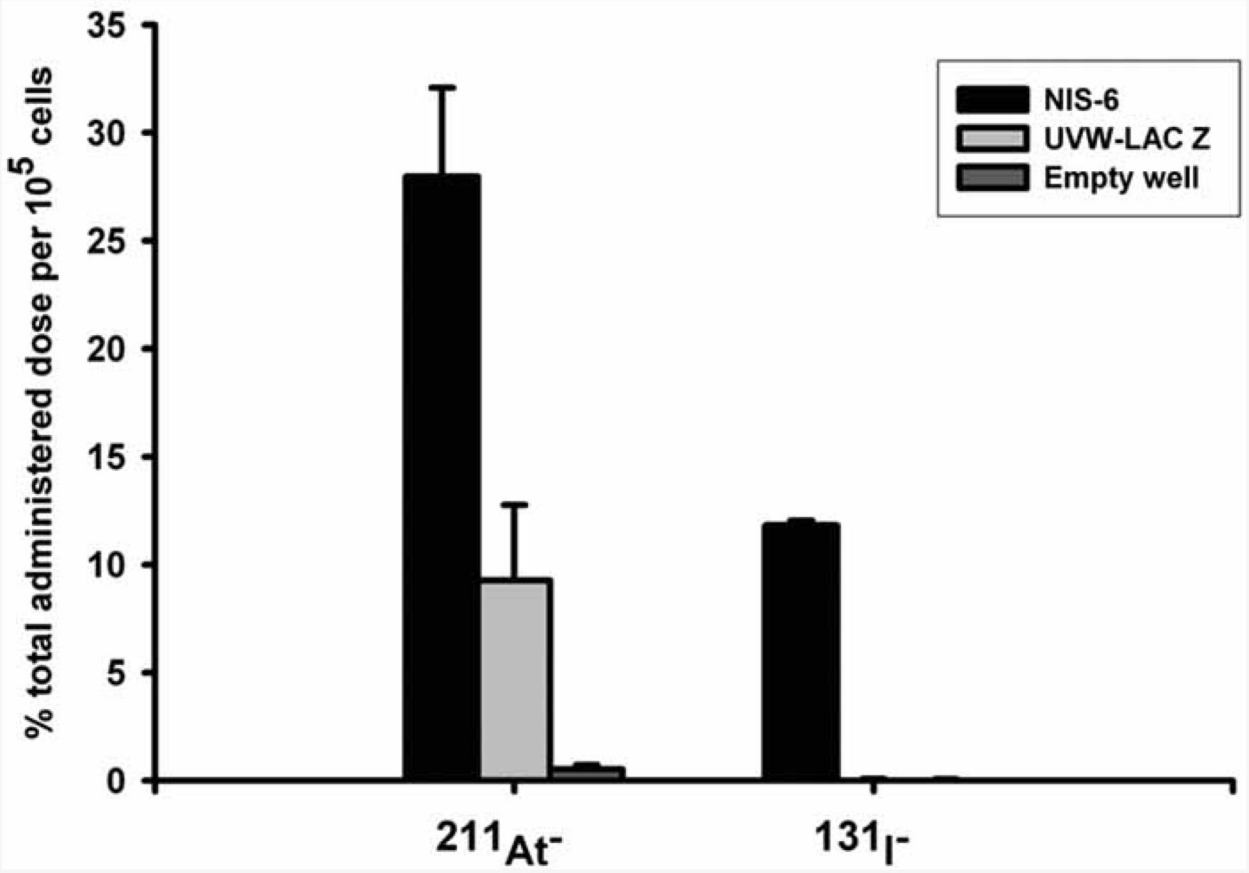

Fig. (2).

NIS expression confers iodide and astatide uptake ability. Uptake of iodide and astatide in UVW cells transfected with cDNA for either the human NIS (NIS 6) or lac-Z (UVW-lac-Z). Results are means ± standard deviation (n = 3). Reprinted from: Carlin *et al.* Sodium-iodide symporter (NIS)-mediated accumulation of [^{211}At]astatide in NIS-transfected human cancer cells. *Nucl. Med. Biol.* **2002**, *29*, 729-739 with permission from Elsevier Ltd.

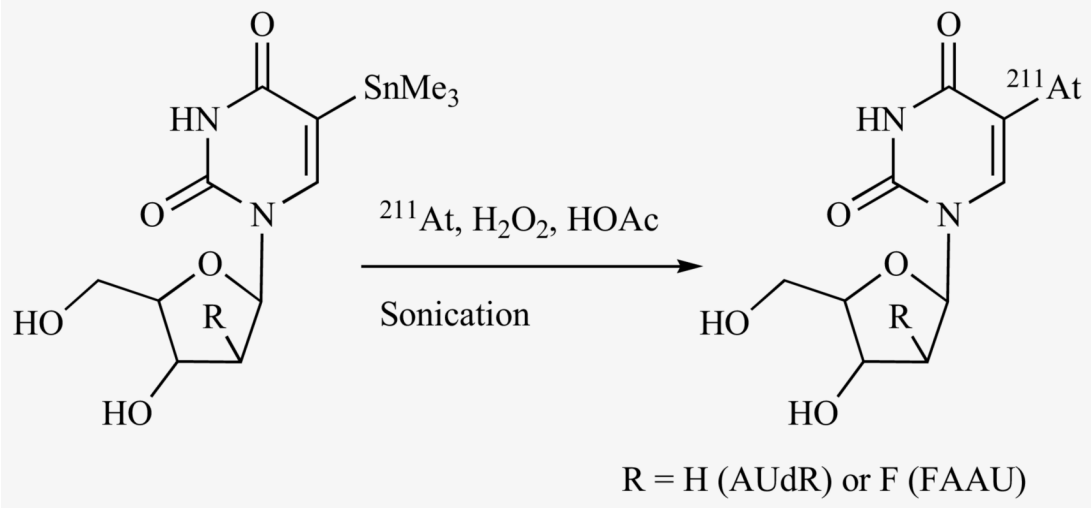

Fig. (3).
Scheme for the synthesis of AUdR and FAAU from the respective tin precursor.

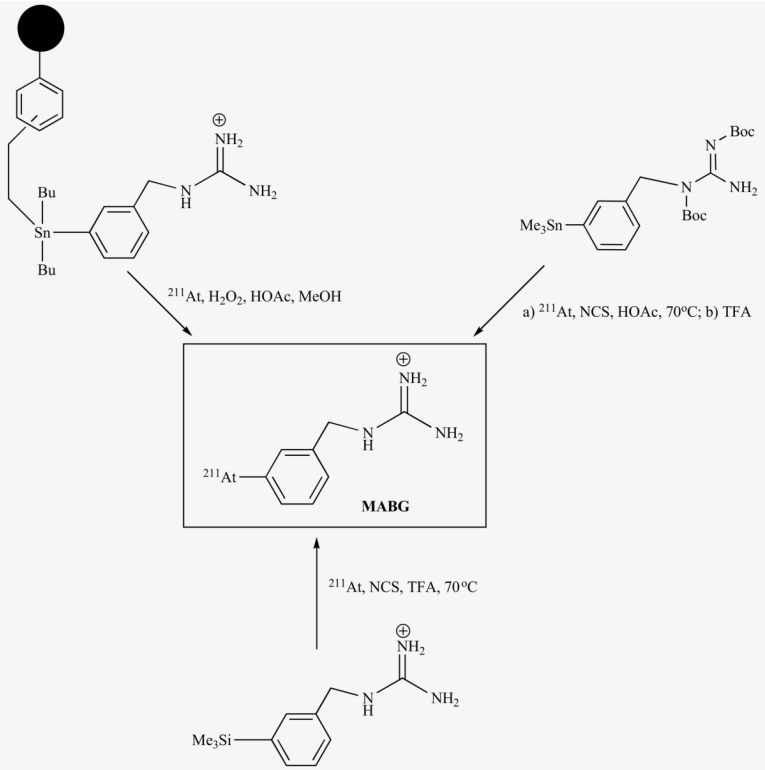

Fig. (4).
Scheme for synthesis of MABG from three different precursors.

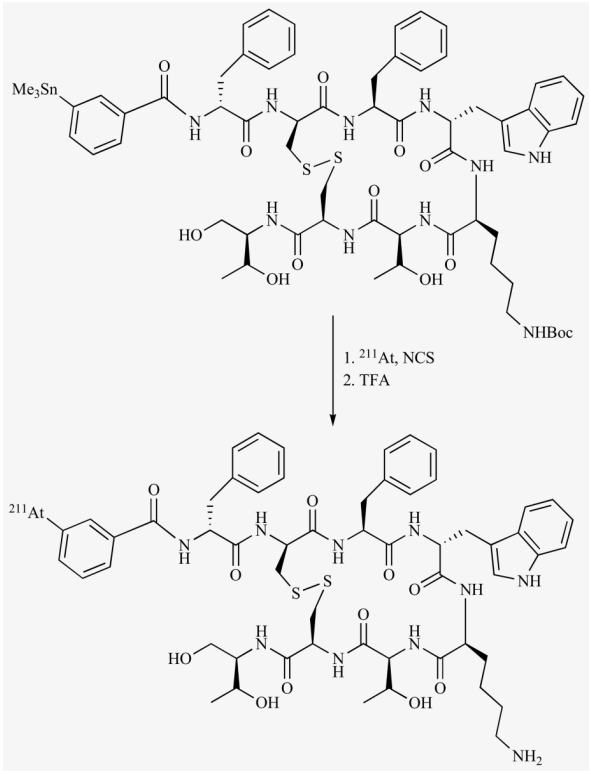

Fig. (5).
Two steps scheme for synthesis of an ^{211}At-labeled octreotide derivative from a tin precursor.

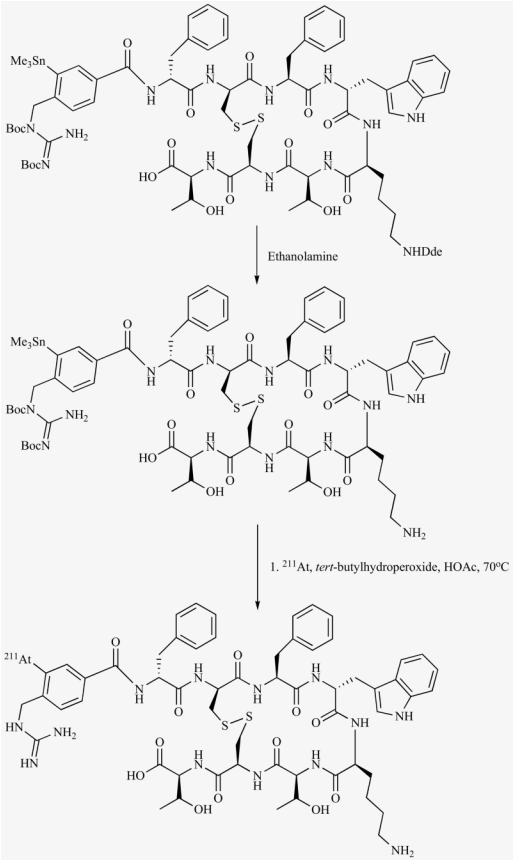

Fig. (6).
Scheme for the synthesis of an ^{211}At-labeled octreotate derivative in a single step from a tin precursor, which was derived *via* an orthogonal protection-deprotection strategy.

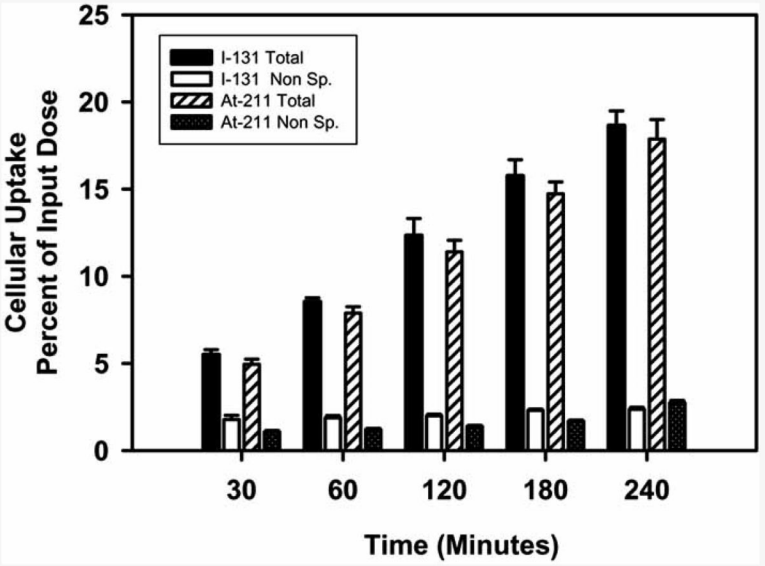

Fig. (7).

Paired-label internalization of ^{211}At- and ^{131}I-labeled octreotate derivative by SSTR-expressing D341 human medulloblastoma cells as a function of time.

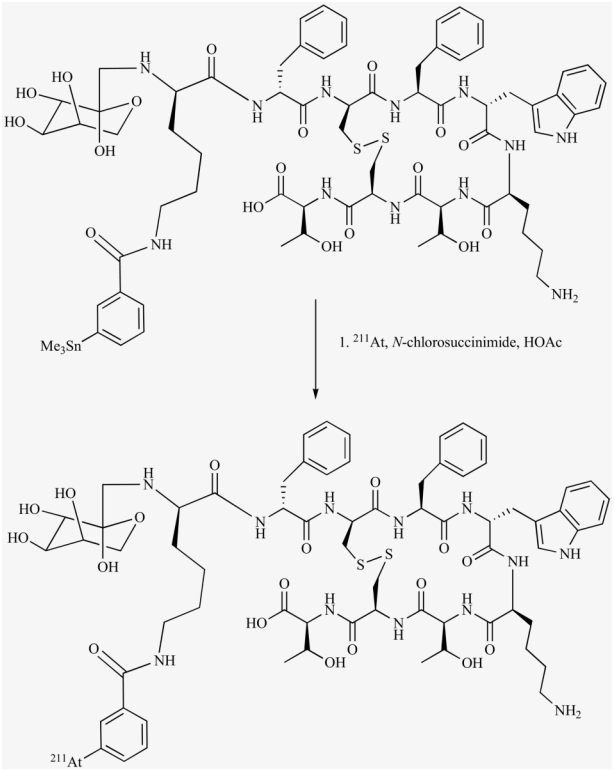

Fig. (8).
Scheme for the synthesis of an ^{211}At-labeled octreotate derivative containing a sugar residue in a single step from a tin precursor.

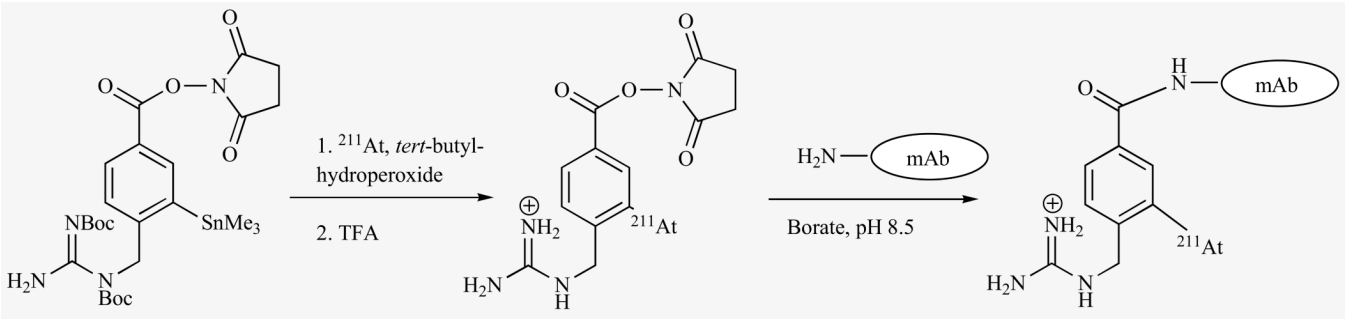

Fig. (9).
Scheme for the synthesis of [^{211}At]SAGMB and its conjugation to a monoclonal antibody.

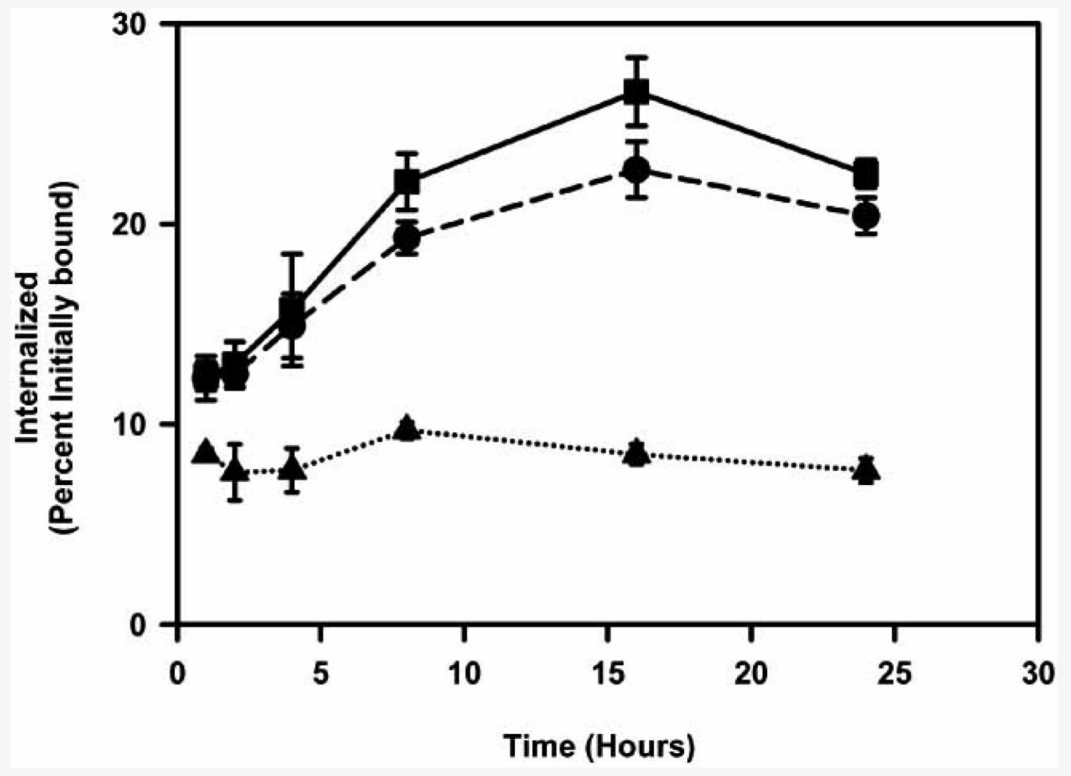

Fig. (10).
Intracellularly trapped radioactivity after U87MG·ΔEGFR cells were incubated with L8A4 radiolabeled with ^{131}I using [^{131}I]SGMIB (square), with ^{125}I using Iodogen (triangle), and with ^{211}At using [^{211}At]SAGMB (circle).

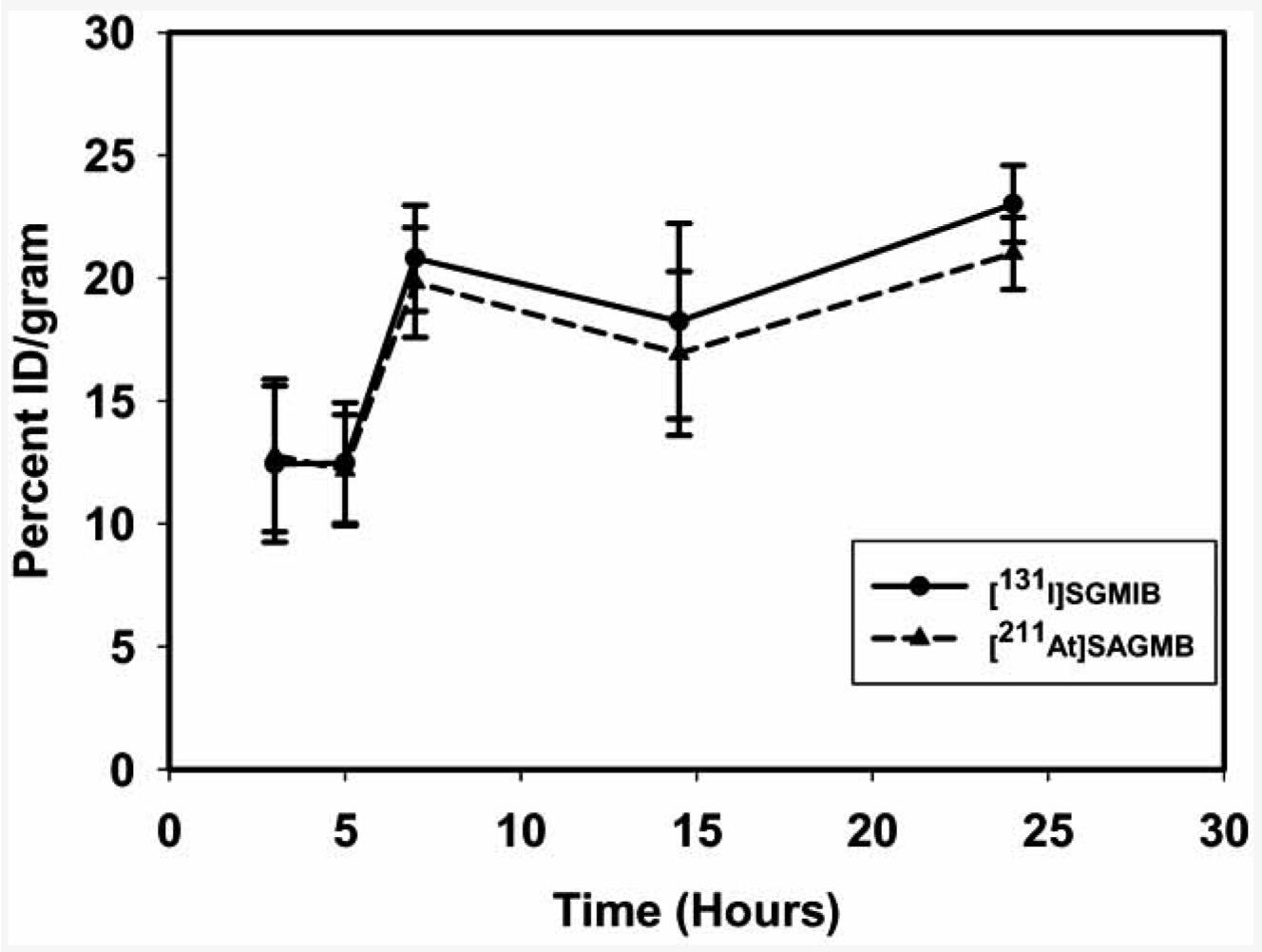

Fig. (11).
Tumor uptake of radioactivity in athymic mice bearing U87MG·EGFR xenografts after administration of L8A4 labeled with ^{211}At and ^{131}I using [^{211}At]SAGMB and [^{131}I]SGMIB, respectively.

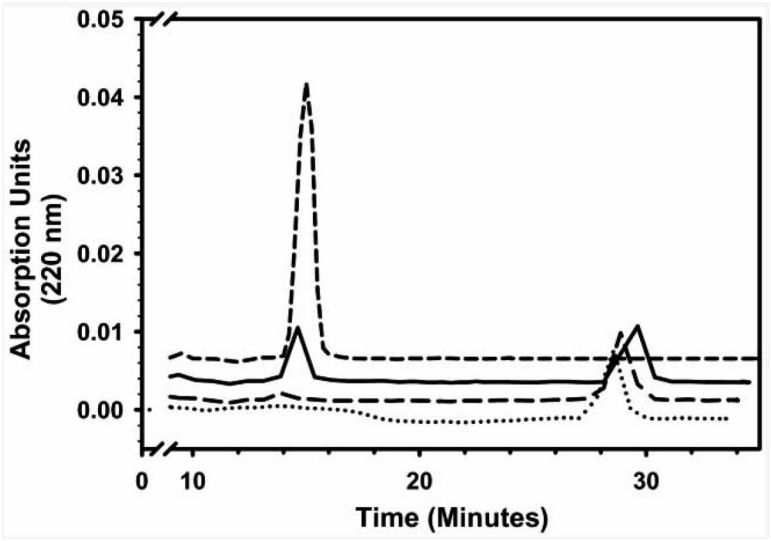

Fig. (12).

Degradation of radiohalogenation precursor BuSTB, after exposure to ^{211}At doses of 644 (——), 1,658 (– – –), and 4,157 Gy (……), followed by normal phase HPLC. For comparison, HPLC profile of control (0 Gy exposure; - - -) is also shown.